Journal of Computational Mathematics
Vol.31, No.6, 2013, 638–662.

http://www.global-sci.org/jcm
doi:10.4208/jcm.1307-m4273

A NEW DIRECT DISCONTINUOUS GALERKIN METHOD WITH SYMMETRIC STRUCTURE FOR NONLINEAR DIFFUSION EQUATIONS*

Chad Vidden Jue Yan
Department of Mathematics, Iowa State University, Ames, IA, USA
E-mail: cvidden@iastate.edu jyan@iastate.edu

Abstract

In this paper we continue the study of discontinuous Galerkin finite element methods for nonlinear diffusion equations following *the direct discontinuous Galerkin (DDG) methods for diffusion problems* [17] and *the direct discontinuous Galerkin (DDG) methods for diffusion with interface corrections* [18]. We introduce a numerical flux for the test function, and obtain a new direct discontinuous Galerkin method with symmetric structure. Second order derivative jump terms are included in the numerical flux formula and explicit guidelines for choosing the numerical flux are given. The constructed scheme has a symmetric property and an optimal $L^2(L^2)$ error estimate is obtained. Numerical examples are carried out to demonstrate the optimal $(k+1)th$ order of accuracy for the method with P^k polynomial approximations for both linear and nonlinear problems, under one-dimensional and two-dimensional settings.

Mathematics subject classification: 65M60.
Key words: Discontinuous Galerkin Finite Element method, Diffusion equation, Stability, Convergence.

1. Introduction

This paper is a continuous study following [17] and [18] regarding a discontinuous Galerkin finite element method for solving time dependent nonlinear diffusion equations of the form

$$U_t - \nabla \cdot (A(U)\nabla U) = 0, \quad (\mathbf{x}, t) \in \Omega \times (0, T), \tag{1.1}$$

where $\Omega \subset \mathbb{R}^d$, the matrix $A(U) = (a_{ij}(U))$ is symmetric and positive definite, and U is an unknown function of $(\mathbf{x}, t)$ with $\mathbf{x} \in \Omega$.

The discontinuous Galerkin (DG) method is a finite element method with discontinuous piecewise function space for the numerical solution and the test functions. Lacking the restrictions of continuities across the computational cells makes these methods extremely flexible. As a result, DG methods have found application in diverse areas. The application of DG methods to hyperbolic problems has been quite successful since it was originally introduced by Reed and Hill [21] in 1973 for neutron transport equations. A major development of the DG method for nonlinear hyperbolic conservation laws was carried out by Cockburn, Shu, etc. We refer to [9–11] for reviews and further references of DG methods for hyperbolic type of PDEs.

However, application of DG method to diffusion problems has been a challenging task because of the subtle difficulty in defining appropriate numerical fluxes for diffusion terms, see

* Received September 27, 2012 / Revised version received May 9, 2013 / Accepted July 9, 2013 / Published online October 18, 2013 /

e.g. [23]. There have been several DG methods suggested in literature for solving diffusion problems. One class is the *interior penalty* (IP) method, which dates back to 1982 as the symmetric interior penalty (SIPG) method by Arnold [1] (also by Baker in [3] and Wheeler in [28]). We also have the Baumann and Oden method [5, 20], the NIPG method [22] and the IIPG method [13]. Another class is the local discontinuous Galerkin (LDG) methods introduced in [12] by Cockburn and Shu (originally proposed by Bassi and Rebay [4] for compressible Navier-Stokes equations). We refer to the unified analysis article [2] in 2002 for different DG methods involving diffusion term and background references for other DG methods. More recent works include those by Van Leer and Nomura in [26], Gassner et al. in [16], Cheng and Shu in [8] and Brenner et al. in [6].

Recently in [17], we develop a direct discontinuous Galerkin (DDG) method for diffusion equations. The scheme is based on the direct weak formulation of (1.1), and a general numerical flux formula for the solution derivative is proposed. An optimal kth order error estimate in an energy norm is obtained with P^k polynomial approximations for linear diffusion equations. However, numerical experiments in [17] show that when measured under L^2 and L^∞ norms, the scheme accuracy is sensitive to the coefficients in the numerical flux formula. That is, for higher order P^k ($k \geq 4$) polynomial approximations it is difficult to identify suitable coefficients in the numerical flux to obtain optimal $(k+1)$th order of accuracy. In [18], extra interface correction terms are introduced into the scheme formulation, and a refined version of the DDG method is obtained. A simpler numerical flux formula is used in [18] and numerically optimal $(k+1)th$ order of accuracy is achieved for any P^k polynomial approximations.

The DDG method [17] and the DDG method with interface corrections [18] are schemes which both lack symmetric properties. Thus it is difficult to obtain L^2 error analysis. In this work, we introduce a numerical flux for the test function derivative and include more interface terms in the scheme formulation. With the same numerical flux formula for the solution derivative and test function derivative, the bilinear form for the diffusion term thus obtained has a symmetric property. This symmetric structure is the key to further prove an optimal $L^2(L^2)$ error estimate for the DG solution. Also, new guidelines for choosing admissible numerical fluxes are given. The symmetric DDG method is not sensitive to the coefficients in the numerical flux formula. There exists a large class of admissible numerical fluxes that lead to the optimal convergence. Compared to the SIPG method [1], the penalty coefficient estimate can be decreased from k^2 to $k^2/4$. One-dimensional and two-dimensional numerical examples are carried out and we obtain $(k+1)th$ optimal order of accuracy with piecewise P^k polynomial approximations for both linear and nonlinear diffusion problems.

In this paper we use uppercase letters to represent the exact solution and lowercase letters to represent the DG numerical solution and test functions. The rest of the paper is organized as follows. In §2, we describe the scheme formulation for the linear and nonlinear one-dimensional diffusion equations, present admissibility and stability results, and establish an energy norm error estimate for the linear case. In §3, extension to two-dimensional diffusion problems is given. The optimal $L^2(L^2)$ error estimate for the linear two-dimensional equation is presented in §4. Finally numerical examples are shown in §5.

2. One-Dimensional Diffusion Equations

2.1. Scheme formulation for 1-D linear diffusion equation

In this section, we present the new discontinuous Galerkin method with the following 1-D

linear diffusion equation

$$U_t - U_{xx} = 0, \ \text{ for } (x,t) \in \Omega \times (0,T), \tag{2.1}$$

associated with initial data $U(x,0) = U_0(x)$ for $x \in \Omega \subset \mathbb{R}$ and periodic boundary condition. Scheme formulation for general nonlinear 1-D diffusion problems is presented in §2.3. Note that it is for simplicity of presentation to consider periodic boundary conditions. The scheme can be easily applied to any well-posed boundary conditions. We use discontinuous Galerkin finite element method for spacial discretization, then couple with strong-stability preserving (SSP) explicit high order TVD Runge-Kutta method [24, 25] for time discretization to formulate the whole scheme. We should mention the scheme is essentially more efficient for problems with small diffusion coefficient, for example the overall convection dominated convection diffusion equations.

First we partition the spatial domain Ω into computational cells $\Omega = \bigcup_{j=1}^{N} I_j$, where $I_j = [x_{j-\frac{1}{2}}, x_{j+\frac{1}{2}}]$, $j = 1, ..., N$. The center of the cell I_j is denoted by $x_j = \frac{1}{2}\left(x_{j-\frac{1}{2}} + x_{j+\frac{1}{2}}\right)$ and the size of the cell is denoted by $\Delta x_j = x_{j+\frac{1}{2}} - x_{j-\frac{1}{2}}$. We have $\Delta x = \max_j \Delta x_j$. We seek numerical solution u in the piecewise polynomial space,

$$\mathbb{V}_{\Delta x}^k := \left\{ v \in L^2(\Omega) : \quad v|_{I_j} \in P^k(I_j), \quad j = 1, \cdots, N \right\},$$

where $P^k(I_j)$ denotes the space of polynomials in I_j of degree at most k. We are now ready to formulate the DG scheme.

Multiply the heat equation (2.1) by any smooth function $V \in H^1(\Omega)$, integrate over I_j, and perform integration by parts to formally obtain,

$$\int_{I_j} U_t V \ dx - U_x V\Big|_{j-1/2}^{j+1/2} + \int_{I_j} U_x V_x \ dx = 0,$$

where

$$U_x V\Big|_{j-1/2}^{j+1/2} = (U_x)_{j+1/2} V_{j+1/2} - (U_x)_{j-1/2} V_{j-1/2}.$$

Here, $(U_x)_{j\pm 1/2}$ and $V_{j\pm 1/2}$ denote the values of U_x and V at $x = x_{j\pm 1/2}$ respectively.

Then, replace smooth function V by a test function $v \in \mathbb{V}_{\Delta x}^k$ and exact solution U by approximate solution $u \in \mathbb{V}_{\Delta x}^k$. Thus, as in [17], we have the original DDG scheme defined as follows: find the unique approximate solution $u \in \mathbb{V}_{\Delta x}^k$ such that for all test functions $v \in \mathbb{V}_{\Delta x}^k$ and for all $1 \le j \le N$, we have that,

$$\int_{I_j} u_t v \ dx - \widehat{u_x} v\Big|_{j-1/2}^{j+1/2} + \int_{I_j} u_x v_x \ dx = 0, \tag{2.2}$$

$$\int_{I_j} u(x,0) v(x) \ dx = \int_{I_j} U_0(x) v(x) \ dx, \tag{2.3}$$

where

$$\widehat{u_x} v\Big|_{j-1/2}^{j+1/2} = (\widehat{u_x})_{j+1/2} v_{j+1/2}^- - (\widehat{u_x})_{j-1/2} v_{j-1/2}^+.$$

This scheme is well defined if the numerical flux $\widehat{u_x}$ is given. Motivated by the solution derivative trace formula of the heat equation with discontinuous initial data, in [17], the numerical flux was introduced as taking the form,

$$\widehat{u_x} = \beta_0 \frac{[u]}{\Delta x} + \overline{u_x} + \beta_1 \Delta x [u_{xx}] + \beta_2 (\Delta x)^3 [u_{xxxx}] + \cdots. \tag{2.4}$$

Note, here and below we adopt the following notation,

$$u^{\pm} = u(x \pm 0, t), \quad [u] = u^{+} - u^{-}, \quad \overline{u} = \frac{u^{+} + u^{-}}{2}. \tag{2.5}$$

The numerical flux $\widehat{u_x}$ approximates U_x and involves the average $\overline{u_x}$ and even order derivatives jumps of u across the cell interfaces $x_{j\pm 1/2}$. The coefficients $\beta_0, \beta_1, \beta_2, \cdots$ are chosen to ensure the stability and convergence of the method. Note, it is easily seen that this numerical flux is both consistent and conservative.

In order to theoretically guarantee optimal rates of convergence in the L^2 norm, a numerical flux term $\widehat{v_x}$ for the test function v is added to the original DDG method (2.2) to create a symmetric scheme. This test function numerical flux is of the same form as $\widehat{u_x}$ given above. The resulting new scheme, known as the symmetric DDG scheme, is formally defined as follows: find the unique approximate solution $u \in \mathbb{V}_{\Delta x}^k$ such that for all test functions $v \in \mathbb{V}_{\Delta x}^k$ and for all $1 \le j \le N$, we have that,

$$\int_{I_j} u_t v dx - \widehat{u_x} v \Big|_{j-1/2}^{j+1/2} + \int_{I_j} u_x v_x dx + ([u]\widehat{v_x})_{j+1/2} + ([u]\widehat{v_x})_{j-1/2} = 0, \tag{2.6}$$

with the numerical flux terms defined as,

$$\begin{cases} \widehat{u_x} = \beta_0 \frac{[u]}{\Delta x} + \overline{u_x} + \beta_1 \Delta x [u_{xx}], \\ \\ \widehat{v_x} = \beta_0 \frac{[v]}{\Delta x} + \overline{v_x} + \beta_1 \Delta x [v_{xx}]. \end{cases} \tag{2.7}$$

Here $\Delta x = \frac{\Delta x_j + \Delta x_{j+1}}{2}$ if the numerical flux is evaluated at the cell interface $x_{j+1/2}$. Notice we drop higher order terms in (2.4) and take a simpler numerical flux formula for $\widehat{u_x}$. An identical numerical flux formula is used for the test function derivative $\widehat{v_x}$. Note numerically we take the test function v to be nonzero only inside the cell I_j, thus only half of the terms in (2.7) contributes to the computation of $\widehat{v_x}$. In a word, the $\widehat{v_x}$ terms can be written out explicitly as the following,

$$\begin{cases} (\widehat{v_x})_{j+1/2} = -\beta_0 \frac{v^-}{\Delta x} + \frac{1}{2}(v_x)^- - \beta_1 \Delta x (v_{xx})^-, \\ \\ (\widehat{v_x})_{j-1/2} = \beta_0 \frac{v^+}{\Delta x} + \frac{1}{2}(v_x)^+ + \beta_1 \Delta x (v_{xx})^+. \end{cases}$$

The $v^{\pm}$ is as defined in (2.5). This completes the definition of the new symmetric DDG method for the linear diffusion equation (2.1). Summing the scheme (2.6) over all cells I_j and introducing the bilinear form,

$$\mathbb{B}(u, v) = \sum_{j=1}^{N} \int_{I_j} u_x v_x \, dx + \sum_{j=1}^{N} (\widehat{u_x}[v])_{j+1/2} + \sum_{j=1}^{N} ([u]\widehat{v_x})_{j+1/2}, \tag{2.8}$$

we obtain the primal weak formulation as the following,

$$\int_{\Omega} u_t v dx + \mathbb{B}(u, v) = 0. \tag{2.9}$$

It can be seen that the bilinear form $\mathbb{B}(u, v)$ has an obvious symmetry. That is, $\mathbb{B}(u, v) = \mathbb{B}(v, u)$. It is this feature which gives this method the name, DDG method with symmetric structure.

Up to now, we have taken the method of lines approach and have left time variable t continuous. After spatial discretization with symmetric DDG method and multiplication of the local inverse mass matrix, the semidiscrete scheme is equivalent to the first order ODE system,

$$u_t = L(u).$$

For time discretization, explicit third order TVD Runge-Kutta method [24, 25] was used to match the accuracy in space. It is given as,

$$\begin{cases} u^{(1)} = u^n + \Delta t L(u^n), \\ u^{(2)} = \frac{3}{4}u^n + \frac{1}{4}(u^{(1)} + \Delta t L(u^{(1)})), \\ u^{n+1} = \frac{1}{3}u^n + \frac{2}{3}(u^{(2)} + \Delta t L(u^{(2)})). \end{cases}$$

One advantage of coupling DG method with explicit scheme is that the mass matrix is locally defined within each computational cell thus there is no global linear system to solve when comparing with the classical finite element method. The DG solution polynomials communicate with its neighbors through the cell boundaries (numerical flux), which gives this method high efficiency with parallel computing, see the reference in the review volume [10]. We should mention in general the symmetric DDG method coupling with explicit TVD Runge-Kutta method is more efficient for small diffusion coefficient problem. For example, it is more efficient for convection dominated problems.

2.2. Admissibility, stability, and error estimates for 1-D case

As for any DG method, the guiding principle for the choice of numerical flux is the stability requirement. For simplicity of presentation, this section will again consider the one-dimensional linear case as in (2.1). As in [17] we adopt the following admissibility criterion.

Definition 2.1. *(Admissibility) We call numerical flux* $\widehat{u_x}$ *in (2.7) admissible if there exists* $\gamma \in (0,1)$, $\alpha > 0$ *such that for any* $u \in \mathbb{V}^k_{\Delta x}$,

$$\gamma \sum_{j=1}^{N} \int_{I_j} (u_x)^2 \, dx + 2 \sum_{j=1}^{N} \widehat{u_x}[u]_{j+1/2} \geq \alpha \sum_{j=1}^{N} \frac{[u]^2_{j+1/2}}{\Delta x}. \tag{2.10}$$

This admissibility ensures the following stability of the symmetric DDG method.

Theorem 2.1. *(Stability) Consider the symmetric DDG scheme* (2.6). *If the numerical flux* (2.7) *is admissible as described in* (2.10), *then we have*

$$\begin{aligned} &\frac{1}{2}\int_\Omega u^2(x,T)dx + (1-\gamma)\int_0^T \sum_{j=1}^{N} \int_{I_j} u_x^2(x,t)dxdt + \alpha \int_0^T \sum_{j=1}^{N} \frac{[u]^2_{j+1/2}}{\Delta x} dt \\ \leq &\frac{1}{2}\int_\Omega u^2(x,0)dx. \end{aligned} \tag{2.11}$$

This can be proved directly by summation over all j of (2.6) with $v = u$, and using the admissibility condition (2.10).

Next, we list the admissibility theorem that provides the guidelines for choosing an admissible numerical flux, namely the suitable β_0 and β_1 in (2.7). The proof of the theorem exclusively depends on the combinatorial properties of the Hilbert matrices. We refer to [27] for details of the proof and some further discussions on numerical flux admissibility.

Theorem 2.2. *(Admissibility) The numerical flux $\widehat{u_x}$ in (2.7) is admissible provided that*

$$2\beta_0 \geq \alpha + \frac{4}{\gamma}\left(\beta_1^2\left(\frac{k^2(k^2-1)^2}{3}\right) - \beta_1\left(\frac{k^2(k^2-1)}{2}\right) + \frac{k^2}{4}\right), \quad \text{for } k \geq 1. \tag{2.12}$$

To minimize β_0, we have

$$\beta_1^* = \frac{3}{4(k^2-1)} \quad \text{and} \quad \beta_0^* = \frac{\alpha}{2} + \frac{1}{2\gamma}\frac{k^2}{4}. \tag{2.13}$$

Here k is the degree of the approximate polynomial space $\mathbb{V}_{\Delta x}^k$. For $k = 0$ we require $\beta_0 = \frac{1}{2}$ for consistency.

The admissibility Theorem 2.2 provides a way to choose suitable β_0 and β_1 in the numerical flux formula (2.7). From (2.12) we see any $(\beta_0,\ \beta_1)$ pair that falls in the parabolic shaded regions in Fig. 2.1 leads to an admissible numerical flux. Take $\alpha = 1, \gamma = \frac{1}{2}$, the minimized (β_0^*, β_1^*) pair of (2.13) is listed in Table 2.1 with $k = 0, \cdots, 10$. For numerical tests in §5, Table 2.1 is used for choosing (β_0, β_1) pairs.

Table 2.1: Minimized admissible (β_0^*, β_1^*) from (2.13).

k	0	1	2	3	4	5	6	7	8	9	10
β_0^*	$\frac{1}{2}$	$\frac{3}{2}$	$\frac{3}{2}$	$\frac{11}{4}$	$\frac{9}{2}$	$\frac{27}{4}$	$\frac{19}{2}$	$\frac{51}{4}$	$\frac{33}{2}$	$\frac{83}{4}$	$\frac{51}{2}$
β_1^*	0	0	$\frac{1}{4}$	$\frac{3}{32}$	$\frac{1}{20}$	$\frac{1}{32}$	$\frac{3}{140}$	$\frac{1}{64}$	$\frac{1}{84}$	$\frac{3}{320}$	$\frac{1}{132}$

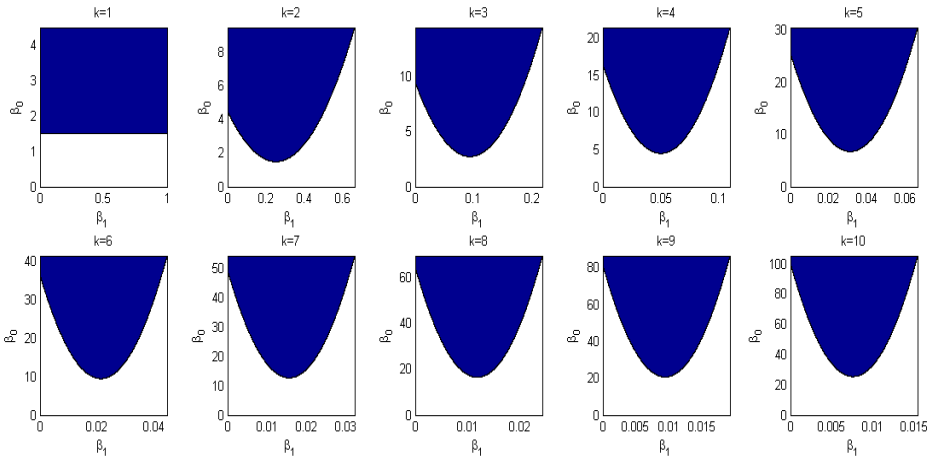

Fig. 2.1. Admissibility region for (β_0, β_1) for $k = 1, 2, \ldots, 10$.

Note that in each $k \geq 2$ case, having β_1 nonzero allows for smaller choice of β_0. Numerical experiments show larger β_0 requires more restrictive CFL conditions on the time step size. Compared to the SIPG method [1], the penalty coefficient ($\sigma = 2\beta_0$ with $\beta_1 = 0$ case) can be decreased from k^2 to four times smaller as $\frac{k^2}{4}$ (here we take $\gamma = 1$ as for the elliptic case). Again k is the polynomial degree of the approximate solution space. The inclusion of second order derivative jumps in the numerical flux seems to play a significant role. We mention that Feng and Wu in [15] also explore the importance of higher order normal derivative jump terms of DG solutions for Helmholtz equations.

Next, we will study the energy norm error estimate for the linear diffusion equation (2.1). Denote the energy norm associated with this scheme as being

$$|||u(\cdot,T)||| := \left(\int_\Omega u^2 \, dx + (1-\gamma) \int_0^T \sum_{j=1}^N \int_{I_j} u_x^2 \, dx d\tau + \alpha \int_0^T \sum_{j=1}^N \frac{[u]_{j+1/2}^2}{\Delta x} \, d\tau \right)^{1/2}, \quad (2.14)$$

with $\gamma \in (0,1)$ and $\alpha > 0$ from (2.10). The form of this energy norm is inspired by the stability estimate (2.11). Before carrying on the error estimate, we first list the following two Lemmas as approximation properties of the finite element space $\mathbb{V}_{\Delta x}^k$ that can be found in finite element textbook, e.g. [7].

Lemma 2.1. *(Approximation property) Let $K \subset \mathbb{R}^n$ be any regular element in the sense that $\rho \Delta x \le diam\,(K) \le \Delta x$ for some constant $0 < \rho < 1$. Let $U \in W^{k+1,p}(\Omega)$ and $\mathbb{P}(U)$ be the L^2 projection of U in $\mathbb{V}_{\Delta x}^k$. Then we have the following approximation property,*

$$||U - \mathbb{P}(U)||_{W^{m,q}(K)} \le c_k (\Delta x)^{n/q - n/p} |U|_{W^{k+1,p}(K)} (\Delta x)^{k+1-m}. \quad (2.15)$$

Here $p, q \in [1, \infty]$, $m \ge 0$ and $k \ge 0$ are integers, and the constant c_k solely depends on k.

Lemma 2.2. *(Inverse inequality) Given the finite dimensional piecewise polynomial space $\mathbb{V}_{\Delta x}^k$, with $1 \le p \le \infty, 1 \le q \le \infty$, $0 \le m \le l \le k$, and a regular element $K \subset \mathbb{R}^n$, there exists C independent of Δx such that for all $v \in \mathbb{V}_{\Delta x}^k$ we have,*

$$\|v\|_{W^{m,q}(K)} \le C \Delta x^{l-m+n/q-n/p} \|v\|_{W^{l,p}(K)}. \quad (2.16)$$

For example, in the following sections we intensively use the inverse inequality estimate with $q = \infty, p = 2, m = 0$ and $n = 2$ as follows,

$$\|v\|_{L^\infty(\partial K)} \le C \Delta x^{l-1} \|v\|_{H^l(K)}.$$

Theorem 2.3. *(Energy norm error estimate in one dimension) Let $e := u - U$ be the error between the exact solution U and the numerical solution u of the symmetric DDG method* (2.6)*. If the numerical flux* (2.7) *is admissible as defined in* (2.10)*, then the energy norm of the error satisfies the inequality,*

$$|||e(\cdot,T)||| \le C |||\partial_x^{k+1} U(\cdot,T)||| (\Delta x)^k, \quad (2.17)$$

where $C = C(k, \gamma, \alpha)$ is a constant depending on k, γ, α but is independent of U and Δx.

Proof. First, rewrite the error as

$$e = u - U = u - \mathbb{P}(U) + \mathbb{P}(U) - U = \mathbb{P}(e) - (U - \mathbb{P}(U)). \quad (2.18)$$

Here $\mathbb{P}(U)$ denotes the L^2 projection of U into $\mathbb{V}_{\Delta x}^k$. That is, $\mathbb{P}(U)$ is the unique function in $\mathbb{V}_{\Delta x}^k$ such that for all $v \in \mathbb{V}_{\Delta x}^k$ and all j,

$$\int_{I_j} (U - \mathbb{P}(U)) v \, dx = 0.$$

Then, with (2.18) we have

$$|||e(\cdot,T)||| \le |||\mathbb{P}(e)(\cdot,T)||| + |||(U - \mathbb{P}(U))(\cdot,T)|||.$$

Using the standard polynomial projection estimate of $\mathbb{V}_{\Delta x}^k$ as in Lemma 2.1 and the definition of the energy norm (2.14), we have,

$$|||(U-\mathbb{P}(U))(\cdot,T)||| \le C|||\partial_x^{k+1}U(\cdot,T)|||(\Delta x)^k.$$

Thus, we only need to find a bound for $|||\mathbb{P}(e)(\cdot,T)|||$. Notice here and below we use capital letter C to represent a generic constant. Define the bilinear form $\mathbb{C}(\cdot,\cdot)$ as,

$$\mathbb{C}(w,v)=\int_0^T\int_\Omega w_t v\ dxdt+\int_0^T\sum_{j=1}^N\int_{I_j} w_x v_x\ dxdt+\Theta(T,w,v),$$

with

$$\Theta(T,w,v)=\int_0^T\sum_{j=1}^N(\widehat{w_x}[v])_{j+1/2}\ dt+\int_0^T\sum_{j=1}^N(\widehat{v_x}[w])_{j+1/2}\ dt.$$

From the scheme definition (2.6), we have $\mathbb{C}(u,v)=0$ and $\mathbb{C}(U,v)=0$ for any test function $v\in\mathbb{V}_{\Delta x}^k$. This implies $\mathbb{C}(e,v)=0$ for all such v as well. With (2.18), then we have that $\mathbb{C}(\mathbb{P}(e),v)=\mathbb{C}(U-\mathbb{P}(U),v)$ for all $v\in\mathbb{V}_{\Delta x}^k$. Taking $v=u-\mathbb{P}(U)=\mathbb{P}(e)$, we then have,

$$\mathbb{C}(\mathbb{P}(e),\mathbb{P}(e))=\mathbb{C}(U-\mathbb{P}(U),\mathbb{P}(e)). \tag{2.19}$$

For the left hand side of (2.19), noting that $\mathbb{P}(e)(\cdot,0)=0$ in addition to the admissibility condition (2.10) for the numerical flux, we obtain,

$$\mathbb{C}(\mathbb{P}(e),\mathbb{P}(e))\ge|||\mathbb{P}(e)(\cdot,T)|||^2-\frac{1}{2}||\mathbb{P}(e)(\cdot,T)||^2_{L^2(\Omega)}. \tag{2.20}$$

Now, turn the attention to the right hand side of (2.19),

$$\begin{aligned}&\mathbb{C}(U-\mathbb{P}(U),\mathbb{P}(e)) \qquad (2.21)\\ &=\int_0^T\int_\Omega(U-\mathbb{P}(U))_t\mathbb{P}(e)\ dxdt+\int_0^T\sum_{j=1}^N\int_{I_j}(U-\mathbb{P}(U))_x\mathbb{P}(e)_x\ dxdt+\Theta(T,U-\mathbb{P}(U),\mathbb{P}(e)),\end{aligned}$$

with

$$\begin{aligned}&\Theta(T,U-\mathbb{P}(U),\mathbb{P}(e))\\ &=\int_0^T\sum_{j=1}^N\Big((\widehat{U-\mathbb{P}(U)})_x[\mathbb{P}(e)]\Big)_{j+1/2}\ dt+\int_0^T\sum_{j=1}^N\Big([U-\mathbb{P}(U)]\widehat{\mathbb{P}(e)}_x\Big)_{j+1/2}\ dt.\end{aligned}$$

For the first term in (2.21), with $\mathbb{P}(e)\in\mathbb{V}_{\Delta x}^k$ we have,

$$\int_0^T\int_\Omega(U-\mathbb{P}(U))_t\mathbb{P}(e)\ dxdt=0.$$

For the second term of (2.21),

$$\begin{aligned}&\int_0^T\sum_{j=1}^N\int_{I_j}(U-\mathbb{P}(U))_x\mathbb{P}(e)_x\ dxdt\\ &\le C|||\partial_x^{k+1}U(\cdot,T)|||^2\Delta x^{2k}+\frac{1-\gamma}{4}\int_0^T\sum_{j=1}^N\|\mathbb{P}(e)_x\|^2_{L^2(I_j)}dt,\end{aligned}$$

here Cauchy inequality and projection error estimate as in Lemma 2.1 are used. For the third term of (2.21), similarly we obtain,

$$\begin{aligned}&\Theta(T, U-\mathbb{P}(U), \mathbb{P}(e))\\ &\leq C|||\partial_x^{k+1}U(\cdot,T)|||^2\Delta x^{2k} + \frac{1-\gamma}{4}\int_0^T \sum_{j=1}^N \|\mathbb{P}(e)_x\|^2_{L^2(I_j)}dt + \frac{\alpha}{2}\int_0^T \sum_{j=1}^N \frac{[\mathbb{P}(e)_x]^2_{j+1/2}}{\Delta x}.\end{aligned}$$

Notice inverse inequalities as in Lemma 2.2 are needed for the above estimate. We refer to [17] and [18] for similar estimates in detail.

Now we have the right hand side of (2.21) as,

$$\begin{aligned}&\mathbb{C}(U-\mathbb{P}(U), \mathbb{P}(e)))\\ &\leq \frac{1}{2}|||\mathbb{P}(e)(\cdot,T)|||^2 - \frac{1}{2}||\mathbb{P}(e)(\cdot,T)||^2_{L^2(\Omega)} + C|||\partial_x^{k+1}U(\cdot,T)|||^2\Delta x^{2k}.\end{aligned}$$

With the left hand side estimate (2.20), we have that $|||\mathbb{P}(e)(\cdot,T)||| \leq C|||\partial_x^{k+1}U(\cdot,T)|||(\Delta x)^k$. The needed result follows. □

Next, the $L^2(L^2)$ *a priori* error estimate is given for the symmetric DDG method (2.6)-(2.7) for the 1-D model equation (2.1). Optimal $(k+1)$th order of accuracy is obtained with P^k polynomial approximations. A complete proof is given for the 2-D linear diffusion equation case in §4. Therefore the proof of the 1-D case is omitted here.

Theorem 2.4. *($L^2(L^2)$ error estimate in one dimension) Consider the 1-D linear model equation* (2.1)*. Let $e := u - U$ be the error between the exact solution U and the numerical solution u of the symmetric DDG method* (2.6)-(2.7)*, we have*

$$\|e\|_{L^2(0,T;L^2)} \leq C\Delta x^{k+1}\left(\|U\|_{L^\infty(0,T;H^{k+1})} + \|U\|_{L^2(0,T;H^{k+1})} + \Delta x\|U_t\|_{L^2(0,T;H^k)}\right).$$

2.3. Scheme formulation for 1-D nonlinear diffusion equations

In this section, we extend the above symmetric DDG scheme to the one-dimensional nonlinear diffusion equation,

$$U_t - (a(U)U_x)_x = 0, \quad \text{for}(x,t) \in \Omega \times (0,T), \tag{2.22}$$

with initial data $U(x,0) = U_0(x)$ and periodic boundary conditions. Here, we assume the diffusion coefficient $a(U) \geq 0$. Also, denote $b(s) = \int a(s)\, ds$. Then, $b(U)_x = a(U)U_x$.

Partition the domain $\Omega = \bigcup_{j=1}^N I_j$ and consider the solution space $\mathbb{V}^k_{\Delta x}$ as above. Then, taking inspiration from the linear case, we have the following scheme. Find the approximate solution $u \in \mathbb{V}^k_{\Delta x}$ of U in (2.22) such that for all test functions $v \in \mathbb{V}^k_{\Delta x}$ and on all I_j, we have,

$$\int_{I_j} u_t v\, dx - \widehat{b(u)_x}v\Big|_{j-1/2}^{j+1/2} + \int_{I_j} b(u)_x v_x\, dx + ([b(u)]\widehat{v_x})_{j+1/2} + ([b(u)]\widehat{v_x})_{j-1/2} = 0,$$

with the numerical fluxes defined as

$$\begin{cases}\widehat{b(u)_x} = \beta_0\frac{[b(u)]}{\Delta x} + \overline{b(u)_x} + \beta_1\Delta x[b(u)_{xx}],\\ \\ \widehat{v_x} = \beta_0\frac{[v]}{\Delta x} + \overline{v_x} + \beta_1\Delta x[v_{xx}].\end{cases} \tag{2.23}$$

Summing over all computational cells I_j provides the primal weak formulation,

$$\int_\Omega u_t v \; dx + \mathbb{B}(b(u), v) = 0,$$

where bilinear form $\mathbb{B}(b(u), v)$ is as given in (2.8). Note, symmetry of this bilinear form is maintained in the sense of $\mathbb{B}(b(u), v) = \mathbb{B}(v, b(u))$ for the nonlinear diffusion equation.

3. Extension to Two-Dimensional Nonlinear Diffusion Equations

In this section we consider the two-dimensional nonlinear parabolic equation,

$$U_t - \nabla \cdot (A(U)\nabla U) = 0, \quad (\mathbf{x}, t) \in \Omega \times (0, T), \tag{3.1}$$

subject to initial data $U(\mathbf{x}, 0) = U_0(\mathbf{x})$ and periodic boundary conditions. The matrix $A(U) = (a_{ij}(U))$ is assumed symmetric positive definite and $\mathbf{x} = (x_1, x_2) \in \Omega \subset \mathbb{R}^2$. Similar to the one-dimensional case, we denote $b_{ij}(U) = \int a_{ij}(U) \; dU$, $i = 1, 2$, $j = 1, 2$.

Let $T_{\Delta\mathbf{x}} = \{K\}$ be a shape-regular partition of the domain Ω with elements K and denote $\Delta\mathbf{x} = \max_K \operatorname{diam}(K)$. As before, define $P^k(K)$ as the space of polynomials in the element K which are of degree at most k. Then, we have the piecewise polynomial numerical solution space as below,

$$\mathbb{V}^k_{\Delta\mathbf{x}} = \{v \in L^2(\Omega) : v\big|_K \in P^k(K), \forall K \in T_{\Delta\mathbf{x}}\}.$$

Along the element boundary ∂K, we use v^{int_K} to denote the value of v evaluated from inside the element K. Correspondingly we use v^{ext_K} to denote the value of v evaluated from outside the element K (inside the neighboring element). The average and jump of v on edge ∂K are defined as

$$\overline{v} = \frac{1}{2}\left(v^{ext_K} + v^{int_K}\right), \quad [v] = v^{ext_K} - v^{int_K}.$$

3.1. Scheme formulation for 2-D linear equation

For sake of presentation, we first consider the case where $A(U) = I$ in (3.1). This gives us the below 2-D heat equation

$$U_t - \Delta U = 0, \quad (\mathbf{x}, t) \in \Omega \times (0, T), \tag{3.2}$$

associated with initial data $U(\mathbf{x}, t = 0) = U_0(\mathbf{x})$ and periodic boundary conditions. As in the 1-D case, multiply the equation by test function, integrate over the computational cell K, perform integration by parts, add interface terms to symmetrize the scheme, and we have the following symmetric DDG scheme formulation. We seek the numerical solution $u \in \mathbb{V}^k_{\Delta\mathbf{x}}$ of U in (3.2) such that for all test functions $v \in \mathbb{V}^k_{\Delta\mathbf{x}}$ and on all elements K we have

$$\int_K u_t v \; d\mathbf{x} + \int_K \nabla u \cdot \nabla v \; d\mathbf{x} - \int_{\partial K} \widehat{u_{\mathbf{n}}} v^{int_K} \; ds + \int_{\partial K} \widehat{v_{\mathbf{n}}}[u] \; ds = 0, \tag{3.3}$$

where the numerical flux at the cell boundary ∂K is defined as

$$\widehat{w_{\mathbf{n}}} = \widehat{\nabla w \cdot \mathbf{n}} = \beta_0 \frac{[w]}{\Delta\mathbf{x}} + \overline{\frac{\partial w}{\partial \mathbf{n}}} + \beta_1 \Delta\mathbf{x}[w_{\mathbf{nn}}]. \tag{3.4}$$

Note, in the numerical flux definition, $\Delta\mathbf{x}$ is the average of the diameter of K and the diameter of its neighboring element. Here $\mathbf{n} = (n_1, n_2)$ is the outward unit normal along the element

boundary ∂K. If the cell boundaries are straight lines, such as for triangular meshes, the numerical flux can be further simplified as

$$\widehat{w_{\mathbf{n}}} = \widehat{w_{x_1}} n_1 + \widehat{w_{x_2}} n_2,$$

with

$$\begin{cases} \widehat{w_{x_1}} = \beta_0 \frac{[w]}{\Delta \mathbf{x}} n_1 + \overline{w_{x_1}} + \beta_1 \Delta \mathbf{x} [w_{x_1 x_1} n_1 + w_{x_2 x_1} n_2], \\ \\ \widehat{w_{x_2}} = \beta_0 \frac{[w]}{\Delta \mathbf{x}} n_2 + \overline{w_{x_2}} + \beta_1 \Delta \mathbf{x} [w_{x_1 x_2} n_1 + w_{x_2 x_2} n_2]. \end{cases}$$

Again, the test function v is taken to be zero outside the element K, thus only one side (inside of K) contributes to the computation of $\widehat{v_{\mathbf{n}}}$ along the element boundary ∂K. Then, as in the 1-D case, we can define a notion of numerical flux admissibility in order to ensure L^2 stability.

Definition 3.1. *(Numerical flux admissibility) We call numerical flux $\widehat{w_{\boldsymbol{n}}}$ admissible if there exists $\gamma \in (0,1)$, $\alpha > 0$ such that for any $w \in \mathbb{V}^k_{\Delta \mathbf{x}}$,*

$$\gamma \sum_{K \in T_\Delta} \int_K |\nabla w|^2 \, d\mathbf{x} + 2 \sum_{K \in T_\Delta} \int_{\partial K} \widehat{w_{\boldsymbol{n}}}[w] \, ds \geq \alpha \sum_{K \in T_\Delta} \int_{\partial K} \frac{[w]^2}{\Delta \mathbf{x}} \, ds. \tag{3.5}$$

This admissibility ensures the following stability of the symmetric DDG method.

Theorem 3.1. *(Stability) Consider the symmetric DDG scheme* (3.3)-(3.4)*. If the numerical flux is admissible as described in* (3.5)*, then we have*

$$\begin{aligned} &\frac{1}{2} \int_\Omega u^2(\mathbf{x}, T) \, d\mathbf{x} + (1-\gamma) \int_0^T \sum_{K \in T_\Delta} \int_K |\nabla u|^2 \, d\mathbf{x} dt + \alpha \int_0^T \sum_{K \in T_\Delta} \int_{\partial K} \frac{[u]^2}{\Delta \mathbf{x}} \, ds dt \\ &\leq \frac{1}{2} \int_\Omega u^2(\mathbf{x}, 0) \, d\mathbf{x}. \end{aligned} \tag{3.6}$$

This can be proved directly by summation over all $K \in T_{\Delta \mathbf{x}}$ of (3.3) with $v = u$ and by using the admissibility condition (3.5). For the 2-D linear model equation (3.2), we have the following optimal energy norm error estimate.

Theorem 3.2. *(Energy norm error estimate in two dimensions) Consider the 2-D linear diffusion equation* (3.2)*. Let $e := u - U$ be the error between the exact solution U and the numerical solution u of the symmetric DDG method* (3.3)-(3.4)*, we have for multiindex α, $|\alpha| = k+1$,*

$$|||u - U||| \leq C |||D^\alpha U(\cdot, T)|||(\Delta \mathbf{x})^k.$$

Here, the energy norm is the analogous two-dimensional form of the one-dimensional case. The proof is similar to the one-dimensional case given in §2.2 and is omitted.

3.2. Scheme formulation for 2-D nonlinear diffusion equations

We consider the fully nonlinear 2-D case as given in (3.1). The scheme formulation is given as follows. We seek approximation $u \in \mathbb{V}^k_{\Delta \mathbf{x}}$ of U in (3.1) such that the following scheme is satisfied for all test functions $v \in \mathbb{V}^k_{\Delta \mathbf{x}}$ on all elements K,

$$\int_K u_t v \, d\mathbf{x} + \int_K \sum_{i,j=1}^2 b_{ij}(u)_{x_j} v_{x_i} \, d\mathbf{x} - \int_{\partial K} \sum_{i,j=1}^2 \widehat{b_{ij}(u)_{x_j}} n_i v^{int_K} \, ds + \int_{\partial K} \sum_{i,j=1}^2 \widehat{v_{x_j}} n_i [b_{ij}(u)] \, ds = 0. \tag{3.7}$$

For $j = 1, 2$, the numerical flux terms are defined as

$$\widehat{b_{ij}(u)_{x_j}} = \beta_0 \frac{[b_{ij}(u)]}{\Delta \mathbf{x}} n_j + \overline{b_{ij}(u)_{x_j}} + \beta_1 \Delta \mathbf{x} [b_{ij}(u)_{x_1 x_j} n_1 + b_{ij}(u)_{x_2 x_j} n_2],$$
$$\widehat{v_{x_j}} = \beta_0 \frac{[v]}{\Delta \mathbf{x}} n_j + \overline{v_{x_j}} + \beta_1 \Delta \mathbf{x} [v_{x_1 x_j} n_1 + v_{x_2 x_j} n_2].$$

Again, in the above numerical flux definition, $\Delta \mathbf{x}$ is the average of the diameter of K and its neighboring element diameter. Notice in the following section regarding $L^2(L^2)$ error analysis, the $\Delta \mathbf{x}$ is considered to be the maximum diameter among all elements.

4. $L^2(L^2)$ Error Estimate for 2-D Linear Diffusion Equation

In this section, we carry out the $L^2(L^2)$ *a priori* error analysis for the symmetric DDG method (3.3)-(3.4) of the two-dimensional linear diffusion equation (3.2). We adopt the same bilinear form notation as the 1-D case (2.8),

$$\mathbb{B}(u, v) = \sum_K \int_K \nabla u \cdot \nabla v \, d\mathbf{x} + \sum_K \int_{\partial K} \widehat{u_{\mathbf{n}}}[v] \, ds + \sum_K \int_{\partial K} [u] \widehat{v_{\mathbf{n}}} \, ds. \tag{4.1}$$

The primal weak formulation is obtained as,

$$\int_\Omega u_t v \, d\mathbf{x} + \mathbb{B}(u, v) = 0. \tag{4.2}$$

In the following theorems, we use letter C to represent a generic constant.

4.1. $L^2(L^2)$ error estimate

Theorem 4.1. *($L^2(L^2)$ error estimate in two dimensions) Consider the 2-D linear diffusion equation* (3.2)*. Let $e := u - U$ be the error between the exact solution U and the numerical solution u of the symmetric DDG method* (3.3)-(3.4)*, we have*

$$\|e\|_{L^2(0,T;L^2(\Omega))} \le C \Delta \mathbf{x}^{k+1} \left(\|U\|_{L^\infty(0,T;H^{k+1}(\Omega))} + \|U\|_{L^2(0,T;H^{k+1}(\Omega))} + \Delta \mathbf{x} \|U_t\|_{L^2(0,T;H^k(\Omega))} \right).$$

Proof. We carry out the proof of the theorem in three steps. First, we apply the below parabolic lift Theorem 4.2 and obtain the following,

$$\begin{aligned}
&\|e\|_{L^2(0,T;L^2(\Omega))} \\
&\le C \Delta \mathbf{x} \left(\|e\|_{L^\infty(0,T;L^2(\Omega))} + \|\nabla e\|_{L^2(0,T;L^2(\Omega))} + \sqrt{\int_0^T \sum_K \int_{\partial K} \frac{[e]^2}{\Delta \mathbf{x}} \, ds dt} \right) \\
&\quad + C \Delta \mathbf{x}^2 \|e_t\|_{L^2(0,T;L^2(\Omega))} + C \Delta \mathbf{x}^{3/2} \sqrt{\int_0^T \sum_K \int_{\partial K} (\overline{e_{\mathbf{n}}})^2 \, ds dt} \\
&\quad + C \Delta \mathbf{x}^{5/2} \sqrt{\int_0^T \sum_K \int_{\partial K} [e_{\mathbf{nn}}]^2 \, ds dt}.
\end{aligned}$$

Second, we apply the time derivative estimate Theorem 4.3 and the interface error estimate Theorem 4.4 to bound the $\|e_t\|_{L^2(0,T;L^2(\Omega))}$ term and the higher derivative interface terms and obtain,

$$\begin{aligned}
&\|e\|_{L^2(0,T;L^2(\Omega))} \\
&\leq C\Delta\mathbf{x}\left(\|e\|_{L^\infty(0,T;L^2(\Omega))} + \|\nabla e\|_{L^2(0,T;L^2(\Omega))} + \left(\int_0^T \sum_K \int_{\partial K} \frac{[e]^2}{\Delta\mathbf{x}}\, dsdt\right)^{1/2}\right) \\
&\quad + C\Delta\mathbf{x}^{k+1}\|U\|_{L^2(0,T;H^{k+1}(\Omega))} + C\Delta\mathbf{x}^{k+2}\|U_t\|_{L^2(0,T;H^k(\Omega))} \\
&\quad + C\Delta\mathbf{x}^{k+1}\|U\|_{L^\infty(0,T;H^{k+1}(\Omega))}.
\end{aligned}$$

Finally, we combine the energy estimate provided by Theorem 3.2 and the above estimate to complete the proof.

4.2. Parabolic lift

The $L^2(L^2)$ error estimate is enhanced to optimal $(k+1)$th order convergence rates through the following parabolic lift theorem.

Theorem 4.2. *(Parabolic lift) Let $e := u - U$ be the error of the symmetric DDG method (3.3)-(3.4). Assume $e \in H^k(K)$, for all elements K. We then have*

$$\begin{aligned}
&\|e\|_{L^2(0,T;L^2(\Omega))} \\
&\leq C\Delta\mathbf{x}\left(\|e\|_{L^\infty(0,T;L^2(\Omega))} + \|\nabla e\|_{L^2(0,T;L^2(\Omega))} + \sqrt{\int_0^T \sum_K \int_{\partial K} \frac{[e]^2}{\Delta\mathbf{x}}\, dsdt}\right) \\
&\quad + C\Delta\mathbf{x}^2\|e_t\|_{L^2(0,T;L^2(\Omega))} + C\Delta\mathbf{x}^{3/2}\sqrt{\int_0^T \sum_K \int_{\partial K} (\overline{e_{\mathbf{n}}})^2\, dsdt} \\
&\quad + C\Delta\mathbf{x}^{5/2}\sqrt{\int_0^T \sum_K \int_{\partial K} [e_{\mathbf{nn}}]^2\, dsdt}
\end{aligned}$$

Proof. Let's consider the following dual (backward) problem,

$$\begin{cases}
-\Phi_t - \Delta\Phi = e, & \mathbf{x} \in \Omega, t \in [0,T], \\
\Phi = 0, & \mathbf{x} \in \partial\Omega, t \in [0,T], \\
\Phi = 0, & \mathbf{x} \in \Omega, t = T.
\end{cases}$$

By dual regularity [14], there exists a unique solution Φ to this backward problem such that the following result holds,

$$\|\Phi\|_{L^\infty(0,T;H^1(\Omega))} + \|\Phi\|_{L^2(0,T;H^2(\Omega))} \leq C\|e\|_{L^2(0,T;L^2(\Omega))}. \tag{4.3}$$

Now rewriting $\|e(\cdot,t)\|_{L^2(\Omega)}$ in terms of Φ, we have,

$$\begin{aligned}
\|e(\cdot,t)\|^2_{L^2(\Omega)} &= \sum_{K\in T_{\Delta\mathbf{x}}} \int_K e^2\, d\mathbf{x} = \sum_K \int_K e\left(-\Phi_t - \Delta\Phi\right)\, d\mathbf{x} \\
&= -\frac{d}{dt}\sum_K \int_K e\Phi\, d\mathbf{x} + \sum_K \int_K e_t\Phi\, d\mathbf{x} + \sum_K \int_K \nabla e\cdot\nabla\Phi\, d\mathbf{x} - \sum_K \int_{\partial K} e\Phi_{\mathbf{n}}\, ds
\end{aligned}$$

$$= -\frac{d}{dt}\sum_K \int_K e\Phi \; d\mathbf{x} + \sum_K \int_K e_t\Phi \; d\mathbf{x} + \sum_K \int_K \nabla e \cdot \nabla\Phi \; d\mathbf{x} + \sum_K \int_{\partial K} \overline{\Phi_{\mathbf{n}}}[e] \; ds$$
$$= -\frac{d}{dt}\sum_K \int_K e\Phi \; d\mathbf{x} + \sum_K \int_K e_t\Phi \; d\mathbf{x} + \mathbb{B}(e,\Phi) - \beta_1\Delta\mathbf{x}\sum_K \int_{\partial K} [\Phi_{\mathbf{nn}}][e] \; ds.$$

The bilinear form $\mathbb{B}(e,\Phi)$ is as defined in (4.1). Notice in the above estimate the last two steps hold true because $\Phi \in H^2(\Omega)$ from the regularity of the dual problem (4.3). By use of the general Sobolev inequality [14], we have $\Phi \in \mathbb{C}^{0,\alpha}$ which implies $[\Phi] = 0$ across cell interfaces. Let $\mathbb{P}(\Phi)$ denote the L^2 projection of Φ into $\mathbb{V}^k_{\Delta\mathbf{x}}$. Since $\mathbb{P}(\Phi) \in \mathbb{V}^k_{\Delta\mathbf{x}}$, from the scheme primal formulation we have, $\langle e_t, \mathbb{P}(\Phi)\rangle + \mathbb{B}(e,\mathbb{P}(\Phi)) = 0$. Here, we use the notation $\langle w, v\rangle = \int_\Omega wv \; d\mathbf{x}$. Now we can formally rewrite $\|e(\cdot,t)\|^2_{L^2(\Omega)}$ as,

$$\begin{aligned}&\|e(\cdot,t)\|^2_{L^2(\Omega)}\\ =&-\frac{d}{dt}\sum_K \langle e,\Phi\rangle_K + \sum_K \langle e_t, \Phi - \mathbb{P}(\Phi)\rangle_K + \mathbb{B}(e,\Phi-\mathbb{P}(\Phi)) - \beta_1\Delta\mathbf{x}\sum_K\int_{\partial K}[\Phi_{\mathbf{nn}}][e]\; ds. \quad (4.4)\end{aligned}$$

Next, let's estimate the terms on the right hand side of (4.4). We first bound (we assume $k \geq 1$ with the approximation polynomial space $\mathbb{V}^k_{\Delta\mathbf{x}}$),

$$\sum_K \langle e_t, \Phi - \mathbb{P}(\Phi)\rangle_K \leq \sum_K \|e_t\|_{L^2(K)}\|\Phi - \mathbb{P}(\Phi)\|_{L^2(K)} \leq C\Delta\mathbf{x}^2\|e_t\|_{L^2(\Omega)}\|\Phi\|_{H^2(\Omega)}.$$

Then we have,

$$\begin{aligned}&\mathbb{B}(e,\Phi-\mathbb{P}(\Phi)) - \beta_1\Delta\mathbf{x}\sum_K\int_{\partial K}[\Phi_{\mathbf{nn}}][e]\; ds\\ =&\sum_K\int_K \nabla e\cdot\nabla(\Phi-\mathbb{P}(\Phi))\; d\mathbf{x} + \sum_K\int_{\partial K}\widehat{e}_{\mathbf{n}}[\Phi-\mathbb{P}(\Phi)]\; ds\\ &+\sum_K\int_{\partial K}\widehat{(\Phi-\mathbb{P}(\Phi))}_{\mathbf{n}}[e]\; ds - \beta_1\Delta\mathbf{x}\sum_K\int_{\partial K}[\Phi_{\mathbf{nn}}][e]\; ds\\ =&I_1+I_2+I_3,\end{aligned}$$

with

$$\begin{aligned}I_1=&\sum_K\int_K \nabla e\cdot\nabla(\Phi-\mathbb{P}(\Phi))\; d\mathbf{x} \leq \sum_K \|\nabla e\|_{L^2(K)}\|\nabla(\Phi-\mathbb{P}(\Phi))\|_{L^2(K)}\\ \leq& C\Delta\mathbf{x}\|\nabla e\|_{L^2(\Omega)}\|\Phi\|_{H^2(\Omega)},\end{aligned}$$

and

$$\begin{aligned}I_2 =& \sum_K\int_{\partial K}\widehat{e}_{\mathbf{n}}[\Phi-\mathbb{P}(\Phi)]\; ds\\ =&\sum_K\int_{\partial K}\left(\frac{\beta_0}{\Delta\mathbf{x}}[e] + \overline{e_{\mathbf{n}}} + \beta_1\Delta\mathbf{x}[e_{\mathbf{nn}}]\right)[\Phi-\mathbb{P}(\Phi)]\; ds\\ \leq&\left(C\beta_0\Delta\mathbf{x}^{1/2}\sqrt{\sum_K\int_{\partial K}[e]^2\; ds} + C\Delta\mathbf{x}^{3/2}\sqrt{\sum_K\int_{\partial K}(\overline{e_{\mathbf{n}}})^2\; ds}\right.\\ &\left.+C\beta_1\Delta\mathbf{x}^{5/2}\sqrt{\sum_K\int_{\partial K}[e_{\mathbf{nn}}]^2\; ds}\right)\|\Phi\|_{H^2(\Omega)}.\end{aligned}$$

For the above I_1 and I_2 estimates, we need Cauchy-Schwarz inequality and the projection error estimate of $\Phi - \mathbb{P}(\Phi)$ (Lemma 2.1). This is illustrated in detail for the term $\int_{\partial K}[e][\Phi - \mathbb{P}(\Phi)]\ ds$ as below.

$$\begin{aligned}
&\int_{\partial K}[e][\Phi - \mathbb{P}(\Phi)]\ ds \\
&\leq \sqrt{\int_{\partial K}[e]^2\ ds}\sqrt{\int_{\partial K}[\Phi - \mathbb{P}(\Phi)]^2\ ds} \leq \Delta \mathbf{x}^{1/2}\|\Phi - \mathbb{P}(\Phi)\|_{L^\infty(K)}\sqrt{\int_{\partial K}[e]^2\ ds} \\
&\leq \Delta \mathbf{x}^{1/2} C\Delta \mathbf{x}\|\Phi\|_{H^2(K)}\sqrt{\int_{\partial K}[e]^2\ ds} \leq C\Delta \mathbf{x}^{3/2}\|\Phi\|_{H^2(K)}\sqrt{\int_{\partial K}[e]^2\ ds}.
\end{aligned}$$

Similarly we can estimate the I_3 term as follows,

$$\begin{aligned}
I_3 &= \sum_K \int_{\partial K} \widehat{(\Phi - \mathbb{P}(\Phi))}_{\mathbf{n}}[e]\ ds - \beta_1 \Delta \mathbf{x}\sum_K \int_{\partial K}[\Phi_{\mathbf{nn}}][e]\ ds \\
&= \frac{\beta_0}{\Delta \mathbf{x}}\sum_K \int_{\partial K}[\Phi - \mathbb{P}(\Phi)][e]\ ds + \sum_K \int_{\partial K}\overline{(\Phi - \mathbb{P}(\Phi))_{\mathbf{n}}}[e]\ ds - \beta_1 \Delta \mathbf{x}\sum_K \int_{\partial K}[\mathbb{P}(\Phi)_{\mathbf{nn}}][e]\ ds \\
&\leq \left(C\beta_0 \Delta \mathbf{x}^{1/2} + C\Delta \mathbf{x}^{1/2} + C\beta_1 \Delta \mathbf{x}^{1/2}\right)\|\Phi\|_{H^2(\Omega)}\left(\sum_K \int_{\partial K}[e]^2\ ds\right)^{1/2}.
\end{aligned}$$

For the last term $[\mathbb{P}(\Phi)_{\mathbf{nn}}][e]$ in the above inequality, we first use inverse inequality (Lemma 2.2 with $m = 2, q = \infty$) to bound $[\mathbb{P}(\Phi)_{\mathbf{nn}}]$ with $||\mathbb{P}(\Phi)||_{H^2(\Omega)}$. Then we rewrite $\|\mathbb{P}(\Phi)\|_{H^2(\Omega)} = \|(\mathbb{P}(\Phi) - \Phi) + \Phi\|_{H^2(\Omega)}$ and use the triangle inequality and the approximation property to obtain the estimate. Finally, apply these bounds to the right hand side of (4.4), and integrate in time from 0 to T we obtain,

$$\|e(\cdot, t)\|^2_{L^2(0,T;L^2(\Omega))} \leq \sum_K \int_K e(\cdot, 0)\Phi(\cdot, 0)\ d\mathbf{x} + C\|\Phi\|_{L^2(0,T;H^2(\Omega))}\Pi,$$

where

$$\begin{aligned}
\Pi =& \Delta \mathbf{x}^2\|e_t\|_{L^2(0,T;L^2(\Omega))} + \Delta \mathbf{x}\|\nabla e\|_{L^2(0,T;L^2(\Omega))} \\
&+ [2\beta_0 + 1 + \beta_1]\,\Delta \mathbf{x}^{1/2}\left(\int_0^T \sum_K \int_{\partial K}[e]^2\ dsdt\right)^{1/2} + \Delta \mathbf{x}^{3/2}\left(\int_0^T \sum_K \int_{\partial K}(\overline{e}_{\mathbf{n}})^2\ dsdt\right)^{1/2} \\
&+ \beta_1 \Delta \mathbf{x}^{5/2}\left(\int_0^T \sum_K \int_{\partial K}[e_{\mathbf{nn}}]^2\ dsdt\right)^{1/2}. \qquad (4.5)
\end{aligned}$$

For the initial term we have,

$$\begin{aligned}
&\sum_K \int_K e(\cdot, 0)\Phi(\cdot, 0)\ d\mathbf{x} \\
&= \sum_K \int_K e(\cdot, 0)(\Phi(\cdot, 0) - \mathbb{P}(\Phi)(\cdot, 0))\ d\mathbf{x} \leq \sum_K \|e(\cdot, 0)\|_{L^2(K)}\|\Phi(\cdot, 0) - \mathbb{P}(\Phi)(\cdot, 0)\|_{L^2(K)} \\
&\leq C\Delta \mathbf{x}\|e(\cdot, 0)\|_{L^2(\Omega)}\|\Phi(\cdot, 0)\|_{H^1(\Omega)} \leq C\Delta \mathbf{x}\|e\|_{L^\infty(0,T;L^2(\Omega))}\|\Phi\|_{L^\infty(0,T;H^1(\Omega))}.
\end{aligned}$$

This implies that

$$\|e\|^2_{L^2(0,T;L^2(\Omega))} \le C\Delta\mathbf{x}\|e\|_{L^\infty(0,T;L^2(\Omega))}\|\Phi\|_{L^\infty(0,T;H^1(\Omega))} + C\|\Phi\|_{L^2(0,T;H^2(\Omega))}\Pi.$$

With the dual regularity result (4.3) we finally obtain,

$$\|e\|_{L^2(0,T;L^2(\Omega))} \le C\Delta\mathbf{x}\|e\|_{L^\infty(0,T;L^2(\Omega))} + C\Pi,$$

where Π is as given in (4.5). □

4.3. Time derivative error estimate and interface error estimate

To finish the $L^2(L^2)$ error estimate, we need to bound the time derivative error term $\|e_t\|_{L^2(0,T;L^2(\Omega))} = \|u_t - U_t\|_{L^2(0,T;L^2(\Omega))}$ as well as the two high order derivative interface terms. Theorem 4.3 provides this for the time derivative term, and Theorem 4.4 considers the two interface terms.

Theorem 4.3. *(Time derivative error estimate) Let $e := u - U$ be the error of the symmetric DDG method* (3.3)-(3.4)*, then we have,*

$$\begin{aligned}&\|e_t\|_{L^2(0,T;L^2)} + \|\nabla e\|_{L^\infty(0,T;L^2)}\\ &\le C\Delta\mathbf{x}^{k-1}\|U\|_{L^2(0,T;H^{k+1})} + C\Delta\mathbf{x}^k\|U\|_{L^\infty(0,T;H^{k+1})} + C\Delta\mathbf{x}^k\|U_t\|_{L^2(0,T;H^k)}.\end{aligned}$$

Proof. As in the energy norm error estimate, we rewrite the error as $e = u - U = u - \mathbb{P}(U) + \mathbb{P}(U) - U = \mathbb{P}(e) - \xi$. For sake of presentation we introduce notation $\xi := U - \mathbb{P}(U)$. Then, again use $\langle v, w\rangle$ to denote the L^2 inner product. From the DDG scheme (3.3), we get that for all $v \in \mathbb{V}^k_{\Delta\mathbf{x}}$,

$$\langle e_t, v\rangle + \mathbb{B}(e, v) = 0,$$

which implies that

$$\langle \mathbb{P}(e)_t, v\rangle + \mathbb{B}(\mathbb{P}(e), v) = \langle \xi_t, v\rangle + \mathbb{B}(\xi, v).$$

The bilinear form $\mathbb{B}(\cdot,\cdot)$ is as defined in (4.1). Choose $v = \mathbb{P}(e)_t \in \mathbb{V}^k_{\Delta\mathbf{x}}$ and we have,

$$\langle \mathbb{P}(e)_t, \mathbb{P}(e)_t\rangle + \mathbb{B}(\mathbb{P}(e), \mathbb{P}(e)_t) = \langle \xi_t, \mathbb{P}(e)_t\rangle + \mathbb{B}(\xi, \mathbb{P}(e)_t). \tag{4.6}$$

After integration in time, the goal will be to bound the left hand side of (4.6) below and the right hand side of (4.6) above to obtain the estimate of $\|\mathbb{P}(e)_t\|_{L^2(0,T;L^2(\Omega))}$. Beginning with the left hand side, we have the terms $\langle \mathbb{P}(e)_t, \mathbb{P}(e)_t\rangle = \|\mathbb{P}(e)_t\|^2_{L^2(\Omega)}$ and

$$\begin{aligned}&\mathbb{B}(\mathbb{P}(e), \mathbb{P}(e)_t)\\ &= \sum_K \int_K \nabla\mathbb{P}(e)\cdot\nabla(\mathbb{P}(e)_t)\ d\mathbf{x} + \sum_K \int_{\partial K} \widehat{\mathbb{P}(e)}_{\mathbf{n}}[\mathbb{P}(e)_t]\ ds + \sum_K \int_{\partial K} \widehat{(\mathbb{P}(e)_t)}_{\mathbf{n}}[\mathbb{P}(e)]\ ds\\ &= \sum_K \int_K \nabla\mathbb{P}(e)\cdot\nabla(\mathbb{P}(e)_t)\ d\mathbf{x} + \frac{2\beta_0}{\Delta\mathbf{x}}\sum_K \int_{\partial K}[\mathbb{P}(e)][\mathbb{P}(e)_t]\ ds + \sum_K \int_{\partial K} \overline{\mathbb{P}(e)}_{\mathbf{n}}[\mathbb{P}(e)_t]\ ds\\ &\quad + \beta_1\Delta\mathbf{x}\sum_K \int_{\partial K}[\mathbb{P}(e)_{\mathbf{nn}}][\mathbb{P}(e)_t]\ ds + \sum_K \int_{\partial K} \overline{(\mathbb{P}(e)_t)}_{\mathbf{n}}[\mathbb{P}(e)]\ ds\\ &\quad + \beta_1\Delta\mathbf{x}\sum_K \int_{\partial K}[(\mathbb{P}(e)_t)_{\mathbf{nn}}][\mathbb{P}(e)]\ ds\\ &= \frac{\partial}{\partial t}(T_1 + T_2 + T_3 + T_4),\end{aligned}$$

where

$$T_1 = \frac{1}{2}\sum_K \int_K |\nabla \mathbb{P}(e)|^2 \, d\mathbf{x}, \quad T_2 = \frac{\beta_0}{\Delta \mathbf{x}} \sum_K \int_{\partial K} [\mathbb{P}(e)]^2 \, ds,$$
$$T_3 = \sum_K \int_{\partial K} \overline{\mathbb{P}(e)}_{\mathbf{n}} [\mathbb{P}(e)] \, ds, \quad T_4 = \beta_1 \Delta \mathbf{x} \sum_K \int_{\partial K} [\mathbb{P}(e)_{\mathbf{nn}}][\mathbb{P}(e)] \, ds.$$

Note, here the symmetry of the bilinear form $\mathbb{B}(\cdot,\cdot)$ is essential to obtain this complete time derivative. We then integrate in time of (4.6) and have the left hand side as,

$$\begin{aligned} &\int_0^t \langle \mathbb{P}(e)_t, \mathbb{P}(e)_t \rangle \, d\tau + \int_0^t \mathbb{B}(\mathbb{P}(e), \mathbb{P}(e)_t) \, d\tau \\ &= \int_0^t \|\mathbb{P}(e)_t\|_{L^2(\Omega)} \, d\tau + \sum_{i=1}^4 T_i(t) - \sum_{i=1}^4 T_i(0). \end{aligned} \tag{4.7}$$

We leave $T_1(t)$ and $T_2(t)$ terms for now because they are positive. For $T_3(t)$ and $T_4(t)$ terms we have

$$\begin{aligned} \Big|T_3(t)\Big| &= \Big| \sum_K \int_{\partial K} \overline{\mathbb{P}(e)}_{\mathbf{n}} [\mathbb{P}(e)] \, ds \Big| \le \epsilon_1 \Delta \mathbf{x} \sum_K \int_{\partial K} (\overline{\mathbb{P}(e)}_{\mathbf{n}})^2 \, ds + \frac{1}{4\epsilon_1} \sum_K \int_{\partial K} \frac{[\mathbb{P}(e)]^2}{\Delta \mathbf{x}} \, ds \\ &\le \epsilon_1 C \|\nabla \mathbb{P}(e)\|^2_{L^2(\Omega)} + \frac{1}{4\epsilon_1} \sum_K \int_{\partial K} \frac{[\mathbb{P}(e)]^2}{\Delta \mathbf{x}} \, ds, \end{aligned}$$

and

$$\begin{aligned} \Big|T_4(t)\Big| &= \Big| \beta_1 \Delta \mathbf{x} \sum_K \int_{\partial K} [\mathbb{P}(e)_{\mathbf{nn}}][\mathbb{P}(e)] \, ds \Big| \\ &\le \epsilon_2 \Delta \mathbf{x} \sum_K \int_{\partial K} \Delta \mathbf{x}^2 [\mathbb{P}(e)_{\mathbf{nn}}]^2 \, ds + \frac{\beta_1^2}{4\epsilon_2} \sum_K \int_{\partial K} \frac{[\mathbb{P}(e)]^2}{\Delta \mathbf{x}} \, ds \\ &\le \epsilon_2 C \|\nabla \mathbb{P}(e)\|^2_{L^2(\Omega)} + \frac{\beta_1^2}{4\epsilon_2} \sum_K \int_{\partial K} \frac{[\mathbb{P}(e)]^2}{\Delta \mathbf{x}} \, ds. \end{aligned}$$

Again, inverse inequalities are used for the above T_3 and T_4 estimates. The constant C solely depends on the polynomial degree of the approximation space $\mathbb{V}^k_{\Delta \mathbf{x}}$. Here we choose small enough ϵ_1 and ϵ_2 to guarantee $\frac{1}{2} - C(\epsilon_1 + \epsilon_2) > 0$. Since, by definition, $\mathbb{P}(e)(0) = u(0) - \mathbb{P}(U(0)) = 0$, thus we have $T_i(0) = 0$ for $i = 1, \cdots, 4$. Now we are ready to obtain a lower bound of (4.7) as follows,

$$\begin{aligned} &\int_0^t \langle \mathbb{P}(e)_t, \mathbb{P}(e)_t \rangle \, d\tau + \int_0^t \mathbb{B}(\mathbb{P}(e), \mathbb{P}(e)_t) \, d\tau \\ &\ge \int_0^t \|\mathbb{P}(e)_t\|^2_{L^2(\Omega)} \, d\tau + \left[\frac{1}{2} - \epsilon_1 C - \epsilon_2 C\right] \|\nabla \mathbb{P}(e)\|^2_{L^2(\Omega)} + \left[\beta_0 - \frac{1}{4\epsilon_1} - \frac{\beta_1^2}{4\epsilon_2}\right] \sum_K \int_{\partial K} \frac{[\mathbb{P}(e)]^2}{\Delta \mathbf{x}} \, ds \\ &\ge \int_0^t \|\mathbb{P}(e)_t\|^2_{L^2(\Omega)} \, d\tau + C \|\nabla \mathbb{P}(e)\|^2_{L^2(\Omega)} + C \sum_K \int_{\partial K} \frac{[\mathbb{P}(e)]^2}{\Delta \mathbf{x}} \, ds. \end{aligned} \tag{4.8}$$

Next, consider the right hand side of (4.6). First we have,

$$\langle \xi_t, \mathbb{P}(e)_t \rangle \le \epsilon_3 \|\mathbb{P}(e)_t\|^2_{L^2(\Omega)} + \frac{1}{4\epsilon_3} \|\xi_t\|^2_{L^2(\Omega)} \le \epsilon_3 \|\mathbb{P}(e)_t\|^2_{L^2(\Omega)} + C \frac{\Delta \mathbf{x}^{2k}}{4\epsilon_3} \|U_t\|^2_{H^k(\Omega)}.$$

We require $U_t \in H^k(\Omega)$ in order for this projection estimate to hold. Also, we have the following,

$$\begin{aligned}
&\mathbb{B}(\xi, \mathbb{P}(e)_t)\\
&= \sum_K \int_K \nabla\xi \cdot \nabla(\mathbb{P}(e)_t)\ d\mathbf{x} + \sum_K \int_{\partial K} \widehat{\xi}_{\mathbf{n}}[\mathbb{P}(e)_t]\ ds + \sum_K \int_{\partial K} \widehat{(\mathbb{P}(e)_t)}_{\mathbf{n}}[\xi]\ ds\\
&= \sum_K \int_K \nabla\xi \cdot \nabla(\mathbb{P}(e)_t)\ d\mathbf{x} + \frac{2\beta_0}{\Delta\mathbf{x}} \sum_K \int_{\partial K} [\xi][\mathbb{P}(e)_t]\ ds + \sum_K \int_{\partial K} \overline{\xi}_{\mathbf{n}}[\mathbb{P}(e)_t]\ ds\\
&\quad + \Delta\mathbf{x}\beta_1 \sum_K \int_{\partial K} [\xi_{\mathbf{nn}}][\mathbb{P}(e)_t]\ ds + \sum_K \int_{\partial K} \overline{(\mathbb{P}(e)_t)}_{\mathbf{n}}[\xi]\ ds + \Delta\mathbf{x}\beta_1 \sum_K \int_{\partial K} [(\mathbb{P}(e)_t)_{\mathbf{nn}}][\xi]\ ds\\
&=: S_1 + S_2 + S_3 + S_4 + S_5 + S_6.
\end{aligned}$$

With the projection error estimate and the inverse inequalities, the estimate of these S_i's are obtained as below.

$$\begin{aligned}
S_1 &= \sum_K \int_K \nabla\xi \cdot \nabla(\mathbb{P}(e)_t)\ d\mathbf{x} \le \Delta\mathbf{x}^2\epsilon_4 \|\nabla(\mathbb{P}(e)_t)\|^2_{L^2(\Omega)} + \frac{1}{4\epsilon_4\Delta\mathbf{x}^2}\|\nabla\xi\|^2_{L^2(\Omega)}\\
&\le \epsilon_4 C\|\mathbb{P}(e)_t\|^2_{L^2(\Omega)} + \frac{C}{4\epsilon_4}\Delta\mathbf{x}^{2k-2}|U|^2_{H^{k+1}(\Omega)},\\
S_2 &= \frac{2\beta_0}{\Delta\mathbf{x}} \sum_K \int_{\partial K} [\xi][\mathbb{P}(e)_t]\ ds \le \sum_K \int_{\partial K} \Delta\mathbf{x}\epsilon_5[\mathbb{P}(e)_t]^2 + \frac{\beta_0^2}{4\epsilon_5\Delta\mathbf{x}^3}[\xi]^2\ ds\\
&\le \epsilon_5 C\|\mathbb{P}(e)_t\|^2_{L^2(\Omega)} + \frac{C\beta_0^2}{4\epsilon_5}\Delta\mathbf{x}^{2k-2}|U|^2_{H^{k+1}(\Omega)},\\
S_3 &= \sum_K \int_{\partial K} \overline{\xi}_{\mathbf{n}}[\mathbb{P}(e)_t]\ ds \le \sum_K \int_{\partial K} \Delta\mathbf{x}\epsilon_6[\mathbb{P}(e)_t]^2 + \frac{1}{4\epsilon_6\Delta\mathbf{x}}(\overline{\xi}_{\mathbf{n}})^2\ ds\\
&\le \epsilon_6 C\|\mathbb{P}(e)_t\|^2_{L^2(\Omega)} + \frac{C}{4\epsilon_6}\Delta\mathbf{x}^{2k-2}|U|^2_{H^{k+1}(\Omega)},\\
S_4 &= \Delta\mathbf{x}\beta_1 \sum_K \int_{\partial K} [\xi_{\mathbf{nn}}][\mathbb{P}(e)_t]\ ds \le \sum_K \int_{\partial K} \Delta\mathbf{x}\epsilon_7[\mathbb{P}(e)_t]^2 + \frac{\Delta\mathbf{x}}{4\epsilon_7}\beta_1^2[\xi_{\mathbf{nn}}]^2\ ds\\
&\le \epsilon_7 C\|\mathbb{P}(e)_t\|^2_{L^2(\Omega)} + \frac{C\beta_1^2}{4\epsilon_7}\Delta\mathbf{x}^{2k-2}|U|^2_{H^{k+1}(\Omega)},\\
S_5 &= \sum_K \int_{\partial K} \overline{(\mathbb{P}(e)_t)}_{\mathbf{n}}[\xi]\ ds \le \sum_K \int_{\partial K} \Delta\mathbf{x}^3\epsilon_8\overline{(\mathbb{P}(e)_t)}^2_{\mathbf{n}} + \frac{1}{4\epsilon_8\Delta\mathbf{x}^3}[\xi]^2\ ds\\
&\le \epsilon_8 C\|\mathbb{P}(e)_t\|^2_{L^2(\Omega)} + \frac{C}{4\epsilon_8}\Delta\mathbf{x}^{2k-2}|U|^2_{H^{k+1}(\Omega)},\\
S_6 &= \Delta\mathbf{x}\beta_1 \sum_K \int_{\partial K} [(\mathbb{P}(e)_t)_{\mathbf{nn}}][\xi]\ ds \le \sum_K \int_{\partial K} \Delta\mathbf{x}^5\epsilon_9[(\mathbb{P}(e)_t)_{\mathbf{nn}}]^2 + \frac{\beta_1^2[\xi]^2}{4\epsilon_9\Delta\mathbf{x}^3}\ ds\\
&\le \epsilon_9 C\|\mathbb{P}(e)_t\|^2_{L^2(\Omega)} + \frac{C\beta_1^2}{4\epsilon_9}\Delta\mathbf{x}^{2k-2}|U|^2_{H^{k+1}(\Omega)}.
\end{aligned}$$

We choose small enough ϵ_i, $i = 3, \cdots, 9$ to balance the left hand side term $\|\mathbb{P}(e)_t\|^2_{L^2}$. Integrate in time, we obtain the upper bound of the right hand side of (4.6) as,

$$\begin{aligned}
&\int_0^t \langle \xi_t, \mathbb{P}(e)_t\rangle\ d\tau + \int_0^t \mathbb{B}(\xi, \mathbb{P}(e)_t)\ d\tau\\
&\le \epsilon \int_0^t \|\mathbb{P}(e)_t\|^2_{L^2(\Omega)}\ d\tau + C\Delta\mathbf{x}^{2k}\|U_t\|^2_{L^2(0,T;H^k(\Omega))} + C\Delta\mathbf{x}^{2k-2}\|U\|^2_{L^2(0,T;H^{k+1}(\Omega))}, \quad (4.9)
\end{aligned}$$

where $\epsilon = \epsilon_3 + C\sum_{i=4}^{9}\epsilon_i$. Then, combining (4.9) with (4.8) we obtain

$$\begin{aligned}&\int_0^t \|\mathbb{P}(e)_t\|^2_{L^2(\Omega)} + \sum_K \int_K |\nabla \mathbb{P}(e)|^2 \, d\mathbf{x} + \sum_K \int_K \frac{[\mathbb{P}(e)]^2}{\Delta \mathbf{x}} \, ds \\ &\leq C\Delta \mathbf{x}^{2k-2}\|U\|^2_{L^2(0,T;H^{k+1})} + C\Delta \mathbf{x}^{2k}\|U_t\|^2_{L^2(0,T;H^k)}.\end{aligned}$$

Recall that $e = \mathbb{P}(e) - \xi$ and make use of the triangle inequality and projection error estimates of $\xi = U - \mathbb{P}(U)$, finally we have,

$$\begin{aligned}&\|e_t\|_{L^2(0,T;L^2)} + \|\nabla e\|_{L^\infty(0,T;L^2)} \\ &\leq C\Delta \mathbf{x}^{k-1}\|U\|_{L^2(0,T;H^{k+1})} + C\Delta \mathbf{x}^k\|U\|_{L^\infty(0,T;H^{k+1})} + C\Delta \mathbf{x}^k\|U_t\|_{L^2(0,T;H^k)}.\end{aligned}$$

Theorem 4.4. *(Interface error estimates) Let $e := u - U$ be the error of the symmetric DDG method* (3.3)-(3.4)*, we have,*

$$\begin{aligned}&\Delta \mathbf{x}^{3/2}\left(\int_0^T \sum_K \int_{\partial K} (\overline{e_{\mathbf{n}}})^2 dsdt\right)^{1/2} \\ &\qquad \leq C\Delta \mathbf{x}^{k+1}\|U\|_{L^2(0,T;H^{k+1}(\Omega))} + C\Delta \mathbf{x}^{k+1}\|U\|_{L^\infty(0,T;H^{k+1}(\Omega))}, \\ &\Delta \mathbf{x}^{5/2}\left(\int_0^T \sum_K \int_{\partial K} [e_{\mathbf{nn}}]^2 dsdt\right)^{1/2} \\ &\qquad \leq C\Delta \mathbf{x}^{k+1}\|U\|_{L^2(0,T;H^{k+1}(\Omega))} + C\Delta \mathbf{x}^{k+1}\|U\|_{L^\infty(0,T;H^{k+1}(\Omega))}.\end{aligned}$$

Proof. These results can be obtained using similar techniques as in the proof of the above theorem. Again we use $\xi = U - \mathbb{P}(U)$ to represent the projection error. We have,

$$\begin{aligned}&\Delta \mathbf{x}^{3/2}\left(\int_0^T \sum_K \int_{\partial K} (\overline{(U-u)_{\mathbf{n}}})^2 \, dsdt\right)^{1/2} \\ &= \Delta \mathbf{x}^{3/2}\left(\int_0^T \sum_K \int_{\partial K} (\overline{(U - \mathbb{P}(U) + \mathbb{P}(U) - u)_{\mathbf{n}}})^2 \, dsdt\right)^{1/2} \\ &\leq \sqrt{2}\Delta \mathbf{x}^{3/2}\left(\int_0^T \sum_K \int_{\partial K} (\overline{\xi_{\mathbf{n}}})^2 \, ds + \sum_K \int_{\partial K} (\overline{\mathbb{P}(e)_{\mathbf{n}}})^2 \, dsdt\right)^{1/2} \\ &\leq C\Delta \mathbf{x}^{3/2}\left(\Delta \mathbf{x}^{k-1/2}\|U\|_{L^2(0,T;H^{k+1}(\Omega))} + \Delta \mathbf{x}^{-1/2}\|\nabla \mathbb{P}(e)\|_{L^2(0,T;L^2(\Omega))}\right) \\ &\leq C\Delta \mathbf{x}^{k+1}\|U\|_{L^2(0,T;H^{k+1}(\Omega))} + C\Delta \mathbf{x}^{k+1}\|U\|_{L^\infty(0,T;H^{k+1}(\Omega))}.\end{aligned}$$

In the last step, results from the energy norm estimate were made use of. The proof of the second interface estimate is similar. □

5. Numerical Examples

In this section, we provide numerical examples to illustrate the performance of the symmetric DDG method. One and two-dimensional linear and nonlinear problems are considered. We

note here that 2-D numerical examples are implemented on rectangular meshes. For each computation, Table 2.1 is used as a guideline for the choice of numerical flux coefficients (β_0, β_1). Note, in all examples the error is measured using the regular L^2 and L^∞ norms in space at end time T. The L^∞ error is obtained by evaluating 200 sample points per cell.

Example 5.1. 1-D linear diffusion equation

$$\begin{cases} U_t - U_{xx} = 0, & x \in [0, 2\pi], \\ U(x, 0) = \sin(x), \end{cases} \tag{5.1}$$

with periodic boundary conditions.

Table 5.1: 1-D linear equation (5.1), P^k polynomial approximations with uniform mesh. $T = 1$.

				Error	Error	Order	Error	Order	Error	Order
				$N = 10$	$N = 20$		$N = 40$		$N = 80$	
β_0	3/2	$k = 2$	L^2	1.92E-03	2.36E-04	3.0	2.93E-05	3.0	3.66E-06	3.0
β_1	1/4		L^∞	3.64E-03	4.70E-04	3.0	5.92E-05	3.0	7.42E-06	3.0
β_0	11/4	$k = 3$	L^2	2.60E-05	1.58E-06	4.0	9.81E-08	4.0	6.12E-09	4.0
β_1	3/32		L^∞	5.87E-05	3.67E-06	4.0	2.32E-07	4.0	1.46E-08	4.0
β_0	9/2	$k = 4$	L^2	6.92E-07	2.07E-08	5.1	6.40E-10	5.0	1.99E-11	5.0
β_1	1/20		L^∞	1.68E-06	5.33E-08	5.0	1.67E-09	5.0	5.23E-11	5.0
				$N = 8$	$N = 12$		$N = 16$		$N = 20$	
β_0	27/4	$k = 5$	L^2	1.86E-07	1.67E-08	5.9	2.99E-09	6.0	7.87E-10	6.0
β_1	1/32		L^∞	3.25E-07	2.97E-08	5.9	5.37E-09	6.0	1.42E-09	6.0
β_0	19/2	$k = 6$	L^2	3.06E-09	1.32E-10	7.7	1.48E-11	7.6	2.81E-12	7.4
β_1	3/140		L^∞	4.84E-09	2.40E-10	7.4	2.97E-11	7.3	6.02E-12	7.2

We use this example to verify the optimal convergence of the symmetric DDG method with three tests. The first is carried out on a uniform mesh. Note, for $k = 0, 1$ in this linear case, the symmetric DDG scheme is the same as the SIPG method, thus we begin with quadratic polynomial approximations. Degree k polynomial approximations with $k = 2, \cdots, 6$ are tested, and optimal $(k + 1)$th orders of convergence are achieved. See Table 5.1 for L^2 and L^∞ errors and orders of convergence. Also, recall that N denotes the total number of computational cells.

Table 5.2: 1-D linear equation (5.1), uniform mesh, P^2 quadratic polynomial approximations. Admissibility test with different (β_0, β_1) pair.

				Error	Error	Order	Error	Order	Error	Order
				$N = 10$	$N = 20$		$N = 40$		$N = 80$	
β_0	9/2	$k = 2$	L^2	1.68E-03	1.75E-04	3.3	2.07E-05	3.1	2.55E-06	3.0
β_1	1/2		L^∞	2.62E-03	3.13E-04	3.1	3.87E-05	3.0	4.83E-06	3.0
β_0	3/2	$k = 2$	L^2	1.92E-03	2.36E-04	3.0	2.93E-05	3.0	3.66E-06	3.0
β_1	1/4		L^∞	3.64E-03	4.70E-04	3.0	5.92E-05	3.0	7.42E-06	3.0
β_0	9/4	$k = 2$	L^2	5.65E-04	7.10E-05	3.0	8.90E-06	3.0	1.11E-06	3.0
β_1	1/8		L^∞	1.04E-03	1.33E-04	3.0	1.66E-05	3.0	2.08E-06	3.0
β_0	171/50	$k = 2$	L^2	2.90E-04	3.61E-05	3.0	4.50E-06	3.0	5.63E-07	3.0
β_1	1/20		L^∞	5.80E-04	7.31E-05	3.0	9.16E-06	3.0	1.15E-06	3.0
β_0	393/100	$k = 2$	L^2	2.59E-04	3.19E-05	3.0	3.97E-06	3.0	4.96E-07	3.0
β_1	1/40		L^∞	5.20E-04	6.50E-05	3.0	8.12E-06	3.0	1.01E-06	3.0

The second test addresses the numerical flux admissibility provided by Theorem 2.2, which is explored computationally. There is a wide range of flux coefficients (β_0, β_1) which are admissible as defined by (2.10). Fig. 2.1 illustrates the admissibility region for (β_0, β_1) pairs with $k = 1, 2, \ldots, 10$. In this test, different β_1 values are selected and the correspondingly smallest admissible β_0 is computed from (2.12) with $\alpha = 1, \gamma = \frac{1}{2}$. We list convergence results for quadratic approximations ($k = 2$) in Table 5.2, and numerically the optimal 3rd order of accuracy is observed for wide range of (β_0, β_1) pairs.

Table 5.3: 1-D linear equation (5.1), P^k approximations on nonuniform mesh. $T = 1$.

				Error	Error	Order	Error	Order	Error	Order
				$N = 18$	$N = 36$		$N = 54$		$N = 72$	
β_0	20	$k = 2$	L^2	1.41E-04	1.79E-05	3.0	5.45E-06	2.9	2.39E-06	2.9
β_1	1/4		L^∞	4.18E-04	5.95E-05	2.8	1.80E-05	2.9	7.68E-06	3.0
β_0	25	$k = 3$	L^2	6.70E-06	4.23E-07	4.0	8.41E-08	4.0	2.68E-08	4.0
β_1	3/32		L^∞	2.22E-05	1.35E-06	4.0	2.75E-07	3.9	8.71E-08	4.0
β_0	25	$k = 4$	L^2	1.02E-07	3.02E-09	5.1	4.00E-10	5.0	9.67E-11	4.9
β_1	1/20		L^∞	3.52E-07	1.12E-08	5.0	1.50E-09	5.0	3.59E-10	5.0

The third test is implemented on a nonuniform mesh. The nonuniform mesh is generated by repeating the pattern $\frac{\Delta x}{5}$, $\frac{3\Delta x}{10}$, and $\frac{\Delta x}{2}$, where $\Delta x = \frac{2\pi}{N}$. Table 5.3 provides the convergence results on such a nonuniform mesh. Note, for this nonuniform mesh it was observed computationally that a larger β_0 was needed for the numerical flux pair. Similar requirement on large β_0 is needed for the SIPG method.

Example 5.2. 1-D nonlinear porous medium equation

$$U_t - (2UU_x)_x = 0, \quad x \in [-12, 12]. \tag{5.2}$$

The exact solution is given by

$$U(x,t) = \begin{cases} (t+1)^{-1/3}\left(3 - \frac{x^2}{12(t+1)^{2/3}}\right), & |x| < 6(t+1)^{1/3}, \\ 0, & |x| \geq 6(t+1)^{1/3}. \end{cases}$$

Table 5.4: 1-D nonlinear porous medium equation (5.2), P^k polynomial approximations, $T = 1$.

				Error	Error	Order	Error	Order	Error	Order
				$N = 40$	$N = 80$		$N = 160$		$N = 320$	
β_0	1/2	$k = 0$	L^2	3.54E-02	1.77E-02	1.0	8.84E-03	1.0	4.42E-03	1.0
β_1	0		L^∞	1.45E-01	7.36E-02	1.0	3.71E-02	1.0	1.87E-02	1.0
β_0	2	$k = 1$	L^2	1.29E-03	3.20E-04	2.0	8.02E-05	2.0	2.00E-05	2.0
β_1	1/80		L^∞	4.69E-03	1.15E-03	2.0	2.92E-04	2.0	7.29E-05	2.0
β_0	2	$k = 2$	L^2	3.25E-05	7.30E-08	8.8	1.49E-09	5.6	1.40E-10	3.4
β_1	1/80		L^∞	4.04E-04	9.48E-07	8.7	3.31E-09	8.2	3.03E-10	3.4

We see that the wave solution travels with finite speed. Accuracy tests are carried out and results are listed in Table 5.4 at final time $T = 1$. We obtain $(k+1)$th order of accuracy with P^k polynomial approximations. Note that errors and orders are computed within domain $[-6, 6]$ where the solution is smooth. In Fig. 5.1 we illustrate the evolution of the symmetric DDG

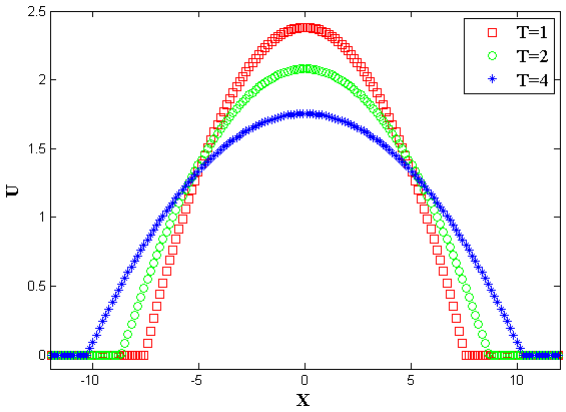

Fig. 5.1. 1-D nonlinear porous medium equation (5.2) at $T = 1, 2, 4$.

solution at times $T = 1, 2, 4$. In each cell, we output the polynomial solution value at the center (symbols) to make up the whole figure. We see the symmetric DDG solution resolves the two kinked corners well with no oscillations.

Example 5.3. 2-D linear diffusion equation

$$\begin{cases} U_t - \epsilon\,(U_{xx} + U_{yy}) = 0, \quad (x, y) \in [0, 2\pi] \times [0, 2\pi], \\ U(x, 0) = \sin(x + y), \end{cases} \tag{5.3}$$

Table 5.5: 2-D linear equation (5.3), P^k approximations with $k = 2, 3, 4$. $T = 5$.

				Error	Error	Order	Error	Order	Error	Order
				$N = 10$	$N = 20$		$N = 30$		$N = 40$	
β_0	3/2	$k = 2$	L^2	6.32E-03	9.13E-04	2.8	2.71E-04	3.0	1.14E-04	3.0
β_1	1/4		L^∞	1.24E-02	1.84E-03	2.7	5.47E-04	3.0	2.30E-04	3.0
β_0	11/4	$k = 3$	L^2	3.74E-04	2.51E-05	3.9	5.01E-06	4.0	1.61E-06	3.9
β_1	3/32		L^∞	2.32E-03	1.24E-04	4.2	2.48E-05	4.0	7.85E-06	4.0
β_0	9/2	$k = 4$	L^2	1.79E-05	5.07E-07	5.1	6.60E-08	5.0	1.56E-08	5.0
β_1	1/20		L^∞	1.01E-04	3.00E-06	5.1	3.93E-07	5.0	9.34E-08	5.0

with periodic boundary conditions and $\epsilon = 0.01$. P^k polynomial approximations are carried out and errors and orders are listed in Table 5.5 with $k = 2, 3, 4$. Optimal convergence is obtained. Note the numerical flux coefficients are chosen according to the 1-D analysis.

Example 5.4. 2-D anisotropic linear diffusion equation

$$\begin{cases} U_t - \epsilon\,(U_{xx} + U_{xy} + U_{yy}) = 0, \quad (x, y) \in [0, 2\pi] \times [0, 2\pi], \\ U(x, 0) = \sin(x + y), \end{cases} \tag{5.4}$$

with $\epsilon = 0.01$. On the rectangular mesh $I_i \times I_j = [x_{i-1/2}, x_{i+1/2}] \times [y_{j-1/2}, y_{j+1/2}]$, the numerical flux for the mixed term should be taken as (according to (3.7)),

$$\widehat{u_x} = \overline{u_x} + \beta_1 \Delta \mathbf{x}[u_{yx}], \quad \text{at} \quad y = y_{j\pm 1/2}.$$

Again, accuracy test is carried out with P^k approximations and errors and orders are listed in Table 5.6 with final time $T = 5$. Optimal $(k+1)$th order of convergence is obtained.

Example 5.5. 2-D nonlinear porous medium equation

$$U_t - (U^2)_{xx} - (U^2)_{yy} = 0, \quad (x, y) \in [-10, 10] \times [-10, 10], \tag{5.5}$$

with zero boundary conditions. The initial condition is given by two bumps as

$$U_0(x, y) = \begin{cases} e^{\frac{-1}{6-(x-2)^2-(y+2)^2}}, & (x-2)^2 + (y+2)^2 < 6, \\ e^{\frac{-1}{6-(x+2)^2-(y-2)^2}}, & (x+2)^2 + (y-2)^2 < 6, \\ 0, & \text{otherwise.} \end{cases}$$

Table 5.6: 2-D anisotropic diffusion equation (5.4), P^k polynomial approximations with $k = 2, 3, 4$.

				Error	Error	Order	Error	Order	Error	Order
				$N = 10$	$N = 20$		$N = 30$		$N = 40$	
β_0	5	$k = 2$	L^2	2.69E-03	3.29E-04	3.0	9.69E-05	3.0	4.08E-05	3.0
β_1	1/12		L^∞	1.87E-02	2.27E-03	3.0	6.68E-04	3.0	2.82E-04	3.0
β_0	5	$k = 3$	L^2	3.11E-04	2.03E-05	3.9	4.11E-06	3.9	1.33E-06	3.9
β_1	1/40		L^∞	2.03E-03	1.30E-04	4.0	2.61E-05	4.0	8.32E-06	4.0
β_0	30	$k = 4$	L^2	1.94E-05	5.54E-07	5.1	7.24E-08	5.0	1.77E-08	4.9
β_1	1/40		L^∞	8.51E-05	2.26E-06	5.2	2.90E-07	5.1	6.91E-08	5.0

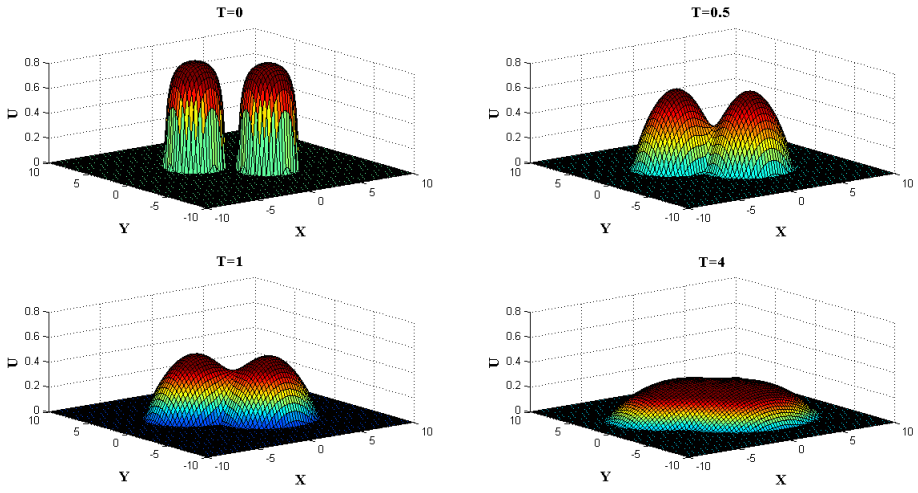

Fig. 5.2. 2-D nonlinear porous medium equation (5.5) at times $T = 0, 0.5, 1.0$, and 4.0.

Piecewise linear approximation with numerical flux coefficients $\beta_0 = \frac{3}{2}$ and $\beta_1 = \frac{1}{10}$ is implemented on a 80×80 rectangular mesh. Note, even though a linear approximation is used, second order jump terms are included within the numerical flux in the scheme formulation (3.7) because of the nonlinearity of the given problem. Results of this test are illustrated in Fig. 5.2 with $T = 0, 0.5, 1.0$, and 4.0. The symmetric DDG solution effectively captures the evolution of the surface with sharp resolution. The results agree well with those in literature, see [19].

Acknowledgments. The research work of the second author is supported by NSF grant DMS-0915247.

References

[1] D.N. Arnold, An interior penalty finite element method with discontinuous elements, *SIAM J. Numer. Anal.*, **19**:4 (1982), 742–760.

[2] D N. Arnold, F. Brezzi, B. Cockburn and L.D. Marini, Unified analysis of discontinuous Galerkin methods for elliptic problems, *SIAM J. Numer. Anal.*, **39**:5 (2001/02), 1749–1779.

[3] G.A. Baker, Finite element methods for elliptic equations using nonconforming elements, *Math. Comp.*, **31** (1977), 45–59.

[4] F. Bassi and S. Rebay, A high-order accurate discontinuous finite element method for the numerical solution of the compressible Navier-Stokes equations, *J. Comput. Phys.*, **131**:2 (1997), 267–279.

[5] C.E. Baumann and J.T. Oden, A discontinuous hp finite element method for convection-diffusion problems, *Comput. Methods Appl. Mech. Engrg.*, **175**:3-4 (1999), 311–341.

[6] S.C. Brenner, L. Owens and L.-Y. Sung, A weakly over-penalized symmetric interior penalty method, *Electron. Trans. Numer. Anal.*, **30** (2008), 107–127.

[7] S.C. Brenner and L.R. Scott, The mathematical theory of finite element methods, volume 15 of Texts in Applied Mathematics, Springer, New York, 3rd. ed., 2008.

[8] Y. Cheng and C.-W. Shu, A discontinuous Galerkin finite element method for time dependent partial differential equations with higher order derivatives, *Math. Comp.*, **77**:262 (2008), 699–730.

[9] B. Cockburn, C. Johnson, C.-W. Shu and E. Tadmor, Advanced numerical approximation of nonlinear hyperbolic equations, volume 1697 of Lecture Notes in Mathematics. Springer-Verlag, Berlin, 1998. Papers from the C.I.M.E. Summer School held in Cetraro, June 2328, 1997, Edited by Alfio Quarteroni, Fondazione C.I.M.E..

[10] B. Cockburn, G.E. Karniadakis, and C.-W. Shu, The development of discontinuous Galerkin methods, In *Discontinuous Galerkin methods* (Newport, RI, 1999), vol. 11 of Lect. Notes Comput. Sci. Eng., pages 3–50. Springer, Berlin, 2000.

[11] B. Cockburn and C.-W. Shu, The local discontinuous Galerkin method for time-dependent convection-diffusion systems, *SIAM J. Numer. Anal.*, **35**(6):2440–2463 (electronic), 1998.

[12] B. Cockburn and C.-W. Shu, Runge-Kutta discontinuous Galerkin methods for convection-dominated problems, *J. Sci. Comput.*, **16**:3 (2001), 173–261.

[13] C. Dawson, S. Sun, and M.F. Wheeler, Compatible algorithms for coupled flow and transport, *Comput. Methods Appl. Mech. Engrg.*, **193**:23-26 (2004) 2565–2580.

[14] L.C. Evans, Partial differential equations, volume 19 of Graduate Studies in Mathematics, American Mathematical Society, Providence, RI, 1998.

[15] X. Feng and H. Wu, Discontinuous Galerkin methods for the Helmholtz equation with large wave number, *SIAM J. Numer. Anal.*, **47**:4 (2009), 2872–2896.

[16] G. Gassner, F. Lorcher and C.D. Munz, A contribution to the construction of diffusion fluxes for finite volume and discontinuous Galerkin schemes, *J. Comput. Phys.*, **224**:2 (2007), 1049–1063.

[17] H. Liu and J. Yan, The direct discontinuous Galerkin (DDG) methods for diffusion problems, *SIAM J. Numer. Anal.*, **47**:1 (2009), 475–698.

[18] H. Liu and J. Yan, The direct discontinuous Galerkin (DDG) method for diffusion with interface corrections, *Commun. Comput. Phys.*, **8**:3 (2010), 541–564.

[19] Y. Liu, C.-W. Shu and M. Zhang, High order finite difference WENO schemes for nonlinear degenerate parabolic equations, *SIAM J. Sci. Comput.*, **33**:2 (2011), 939–965.

[20] J.T. Oden, I. Babuska and C.E. Baumann, A discontinuous hp finite element method for diffusion problems, *J. Comput. Phys.*, **146**:2 (1998), 491–519.

[21] W.H. Reed and T.R. Hill, Triangular mesh methods for the neutron transport equation, *Technical Report Tech*, Report LA-UR-73-479, Los Alamos Scientific Laboratory, 1973.

[22] B. Riviere, M.F. Wheeler and V. Girault, A priori error estimates for finite element methods based on discontinuous approximation spaces for elliptic problems, *SIAM J. Numer. Anal.*, **39**:3 (2001), 902–931.

[23] C.-W. Shu, Different formulations of the discontinuous galerkin method for the viscous terms, *Advances in Scientific Computing*, Z.-C. Shi, M. Mu, W. Xue and J. Zou, editors, Science Press, China, 2001, pp. 144–155.

[24] C.-W. Shu and S. Osher, Efficient implementation of essentially nonoscillatory shock-capturing schemes, *J. Comput. Phys.*, **77**:2 (1988), 439–471.

[25] C.-W. Shu and S. Osher, Efficient implementation of essentially nonoscillatory shock-capturing schemes. II, *J. Comput. Phys.*, **83**:1 (1989), 32–78.

[26] B. van Leer and S. Nomura, Discontinuous Galerkin for diffusion, *Proceedings of 17th AIAA Computational Fluid Dynamics Conference* (June 6 2005), AIAA-2005-5108.

[27] C. Vidden, The Direct Discontinuous Galerkin Method with Symmetric Structure for Diffusion Problems, Iowa State University, Thesis (2012).

[28] M.F. Wheeler, An elliptic collocation-finite element method with interior penalties, *SIAM J. Numer. Anal.*, **15** (1978), 152–161.